Allelic Effects on Uromodulin Aggregates Drive Autosomal Dominant Tubulointerstitial Kidney Disease

Appendix

Table of contents

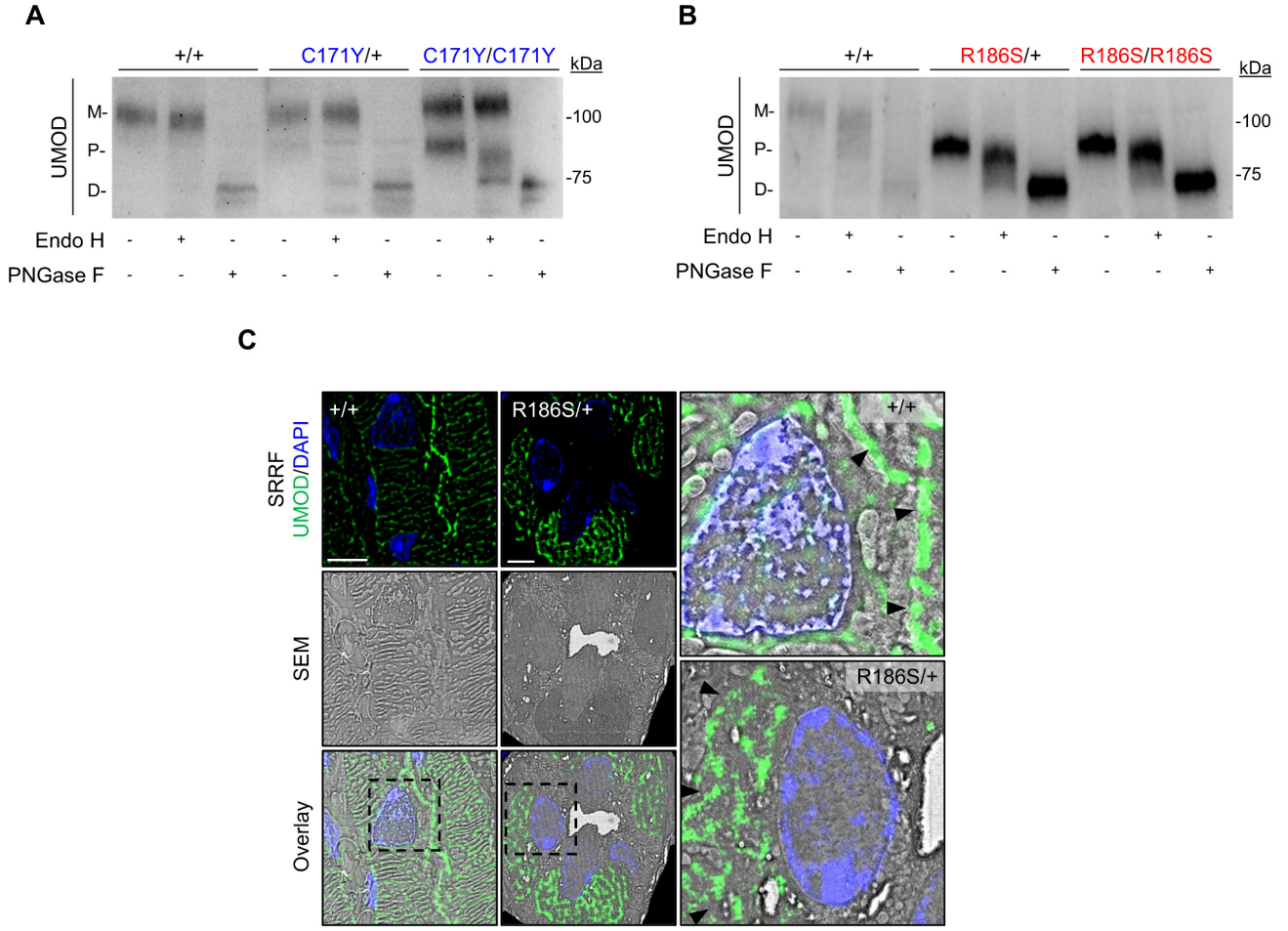

Appendix Figure S1: Uromodulin characteristics in the C171Y and R186S mouse models.

(**A-B**) Immunoblot analysis of UMOD following Endo H or PNGase F treatment in kidneys from 1-month-old C171Y (**A**) and R186S (**B**) mice. M: mature; P: precursor; D: deglycosylated. (**C**) Correlative Light Electron Microscopy (CLEM) of UMOD (green) on kidney sections from 3-month-old +/+ and R186S/+ mice. Nuclei are counterstained with DAPI (blue). Black arrowheads indicate UMOD localization (apical plasma membrane in +/+, endoplasmic reticulum in R186S/+). Scale bar: 5 µm. SRRF, super-resolution radial fluctuation; SEM, scanning electron microscopy.

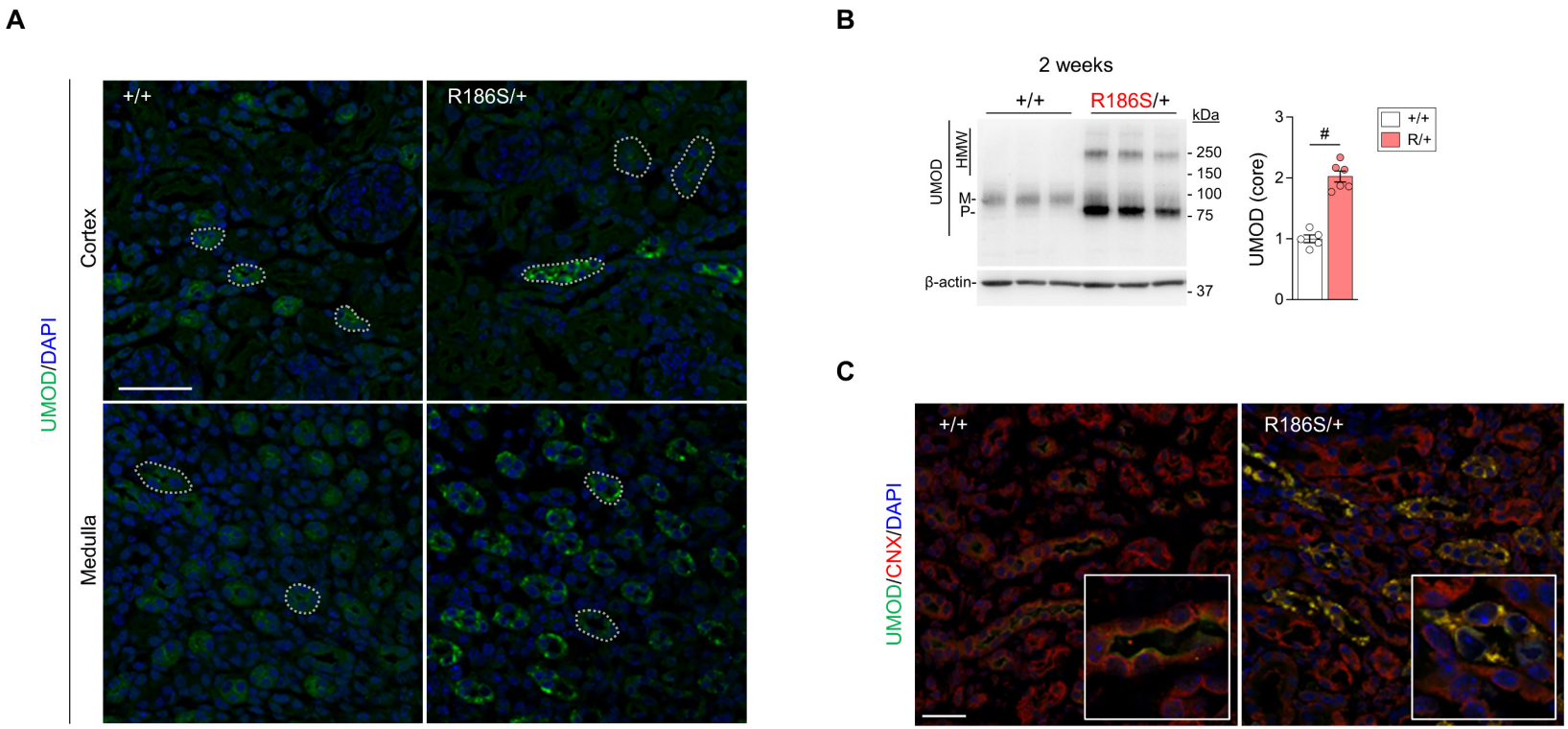

Appendix Figure S2: Early uromodulin processing defects in R186S/+ mice.

(A) Representative immunofluorescence analysis of UMOD (green) on kidney sections from 2-week-old +/+ and R186S/+ mice. Nuclei counterstained with DAPI (blue). Scale bar: 25 µm. Dotted lines identify different tubules with apical or intracellular UMOD accumulation.

(**B**) Representative immunoblot of UMOD in whole kidney samples from 2-week-old +/+ and R186S/+ mice (n=5 to 6 animals per group). β-actin used as loading control. M: mature UMOD; P: premature UMOD; HMW: high molecular weight. Densitometry analysis relative to +/+. Bars indicate mean ± SEM. Unpaired two-tailed t test, $^{\#}P<0.0001$.

(**C**) Representative immunofluorescence analysis of UMOD (green) and CNX (red) on kidney sections from 2-week-old mice. Nuclei are counterstained with DAPI (blue). Scale bar: 25 µm.

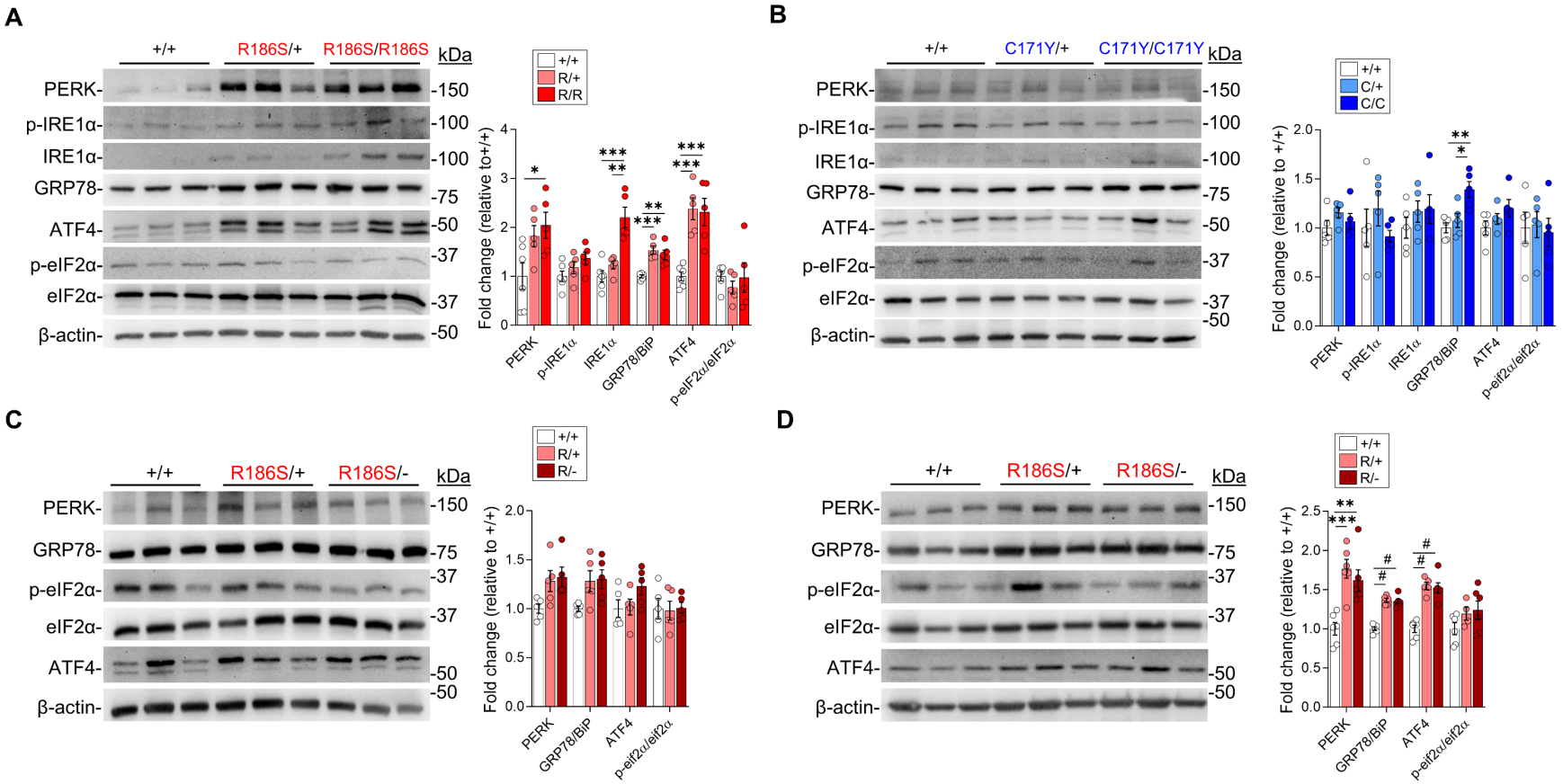

Appendix Figure S3: Unfolded protein response in kidneys from *Umod* KI mice.

(**A-B**) Representative immunoblot analysis of ER stress markers in medulla-enriched kidney fractions from 4-months-old R186S (**A**) and C171Y (**B**) mice (n=5 to 6 animals per group).
(**A**) PERK: $^{*}P$=0.0311; IRE1α: $^{**}P$=0.0011, $^{***}P$=0.0001; GRP78/BiP: $^{***}P$=0.0009, $^{**}P$=0.0040; ATF4: $^{***}P$(+/+ vs. R/+)=0.0008, $^{***}P$(+/+ vs. R/R)=0.0012. (**B**) GRP78/BiP: $^{*}P$=0.019, $^{**}P$=0.0049.
(**C-D**) Representative immunoblot analysis of ER stress markers in 1-month-old medulla-enriched kidney fractions (**C**) or 4-months-old total kidney lysates from +/+, R186S/+ and R186S/- mice (n=5 to 6 animals per group). β-actin used as loading control. Densitometry analysis is relative to +/+.
(**D**) PERK: $^{***}P$=0.0007, $^{**}P$=0.0045; $^{\#}P$<0.0001.
Bars indicate mean ± SEM. One-way ANOVA followed by Tukey's post-hoc test.

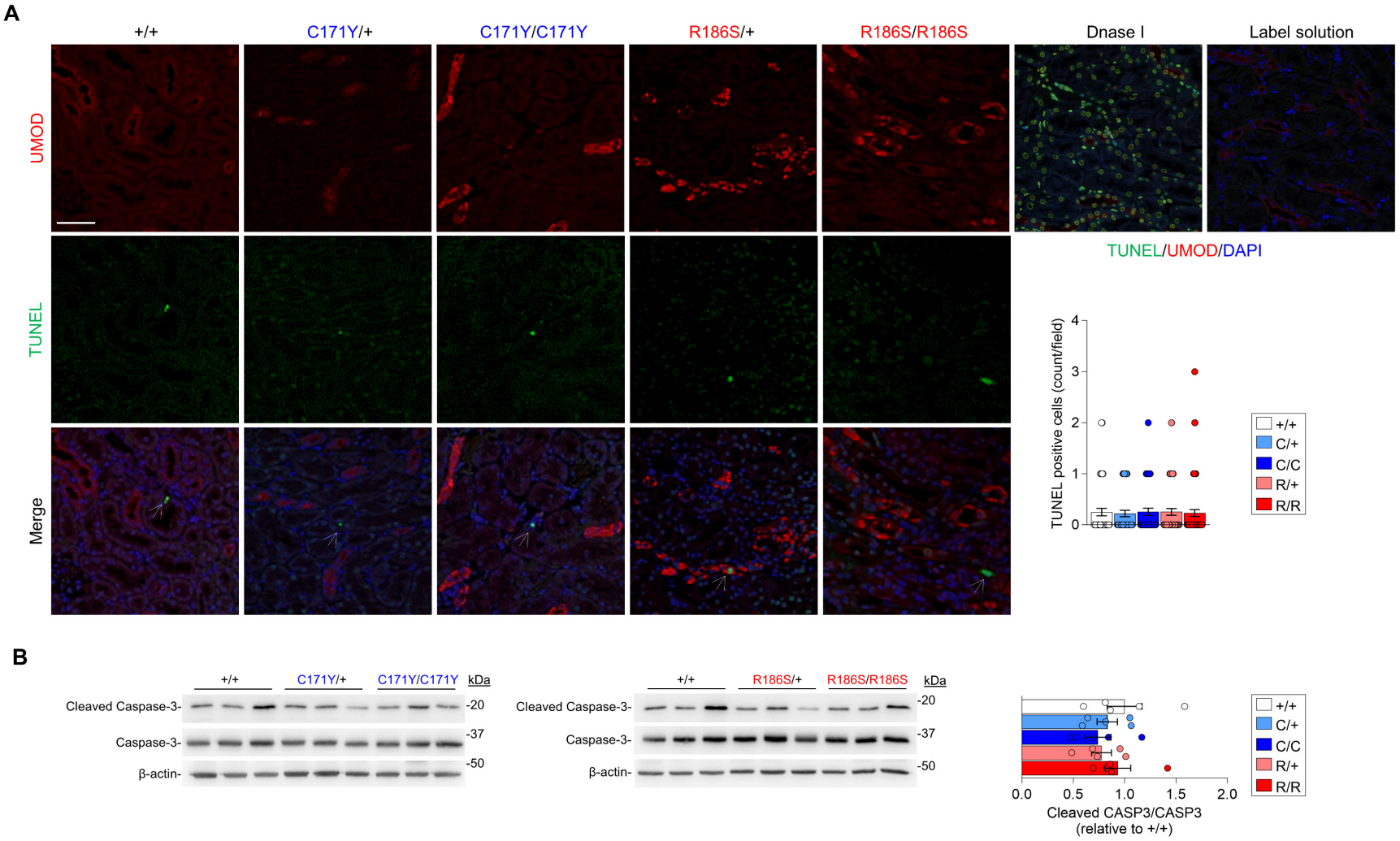

Appendix Figure S4: Lack of apoptosis or caspase activation in *Umod* KI kidneys.

(**A**) Immunofluorescence analysis of TUNEL (green) and UMOD (red) in kidney sections from 4-month-old *Umod* mutant (n ≥ 45 fields from 3-5 kidneys per condition). Nuclei are counterstained with DAPI (blue). Positive control incubated with DNase I and negative control incubated with label solution shown on right panel. Scale bar: 50 µm. Each point of the quantification represents the number of TUNEL+ cells in one field.

(**B**) Representative immunoblot analysis of caspase-3 (CASP3) and cleaved caspase-3 in whole kidney lysates from 4-month-old +/+, C171Y/+ and C171Y/C171Y mice (left) or +/+, R186S/+ and R186S/R186S mice (right). β-actin used as a loading control. Densitometry analysis is relative to +/+.

Bars indicate mean ± SEM. One-way ANOVA followed by Tukey's post-hoc test, (n = 5 animals per group).

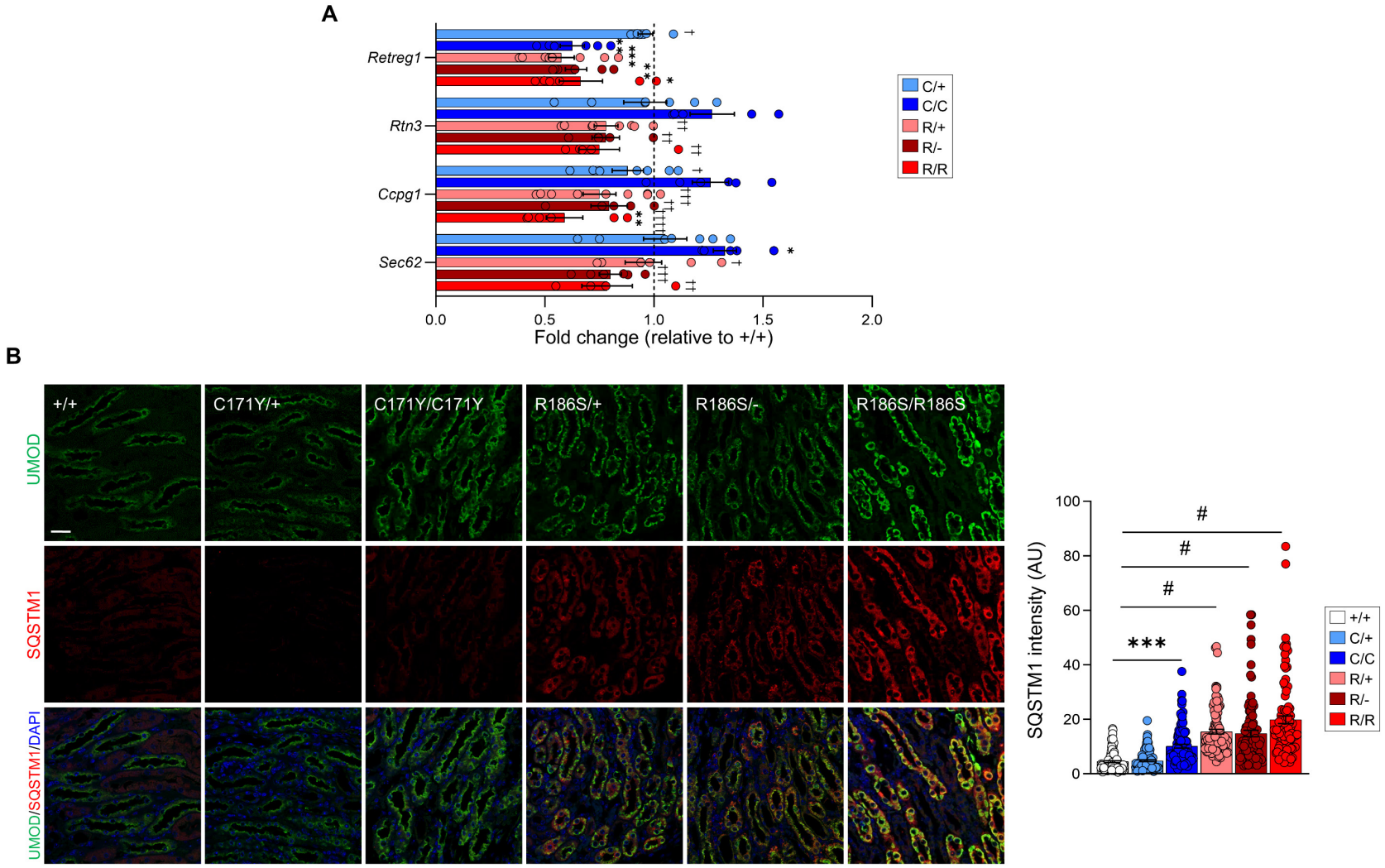

Appendix Figure S5: Mutant UMOD degradation relies on mutation-specific mechanisms.

(**A**) RT-qPCR analysis of ER-phagy genes in *Umod* KI kidneys (n=4 to 9 animals per group). Values are expressed as relative to +/+ (black dotted line).
Retreg1: $^{**}P$(+/+ vs. C/C)=0.0038, $^{***}P$ = 0.0004, $^{**}P$(+/+ vs. R/-)=0.0061, $^{*}P$=0.0113, $^{\dagger}P$=0.0114; *Rtn3*: $^{\dagger\dagger}P$(C/C vs. R/+)=0.0012, $^{\dagger\dagger}P$(C/C vs. R/-)=0.004, $^{\dagger\dagger}P$(C/C vs. R/R)=0.0021; *Ccpg1*: $^{**}P$=0.0059, $^{\dagger}P$=0.0127, $^{\dagger\dagger\dagger}P$=0.0002, $^{\dagger\dagger}P$=0.0015, $^{\dagger\dagger\dagger\dagger}P$<0.0001; *Sec62*: $^{*}P$=0.0494, $^{\dagger}P$=0.016, $^{\dagger\dagger\dagger}P$=0.0006, $^{\dagger\dagger}P$=0.0016.
(**B**) Representative immunofluorescence analysis of UMOD (green) and SQSTM1 (red) on kidney sections from 1-month-old *Umod* KI mice. Nuclei are counterstained with DAPI (blue). Scale bar: 25 µm, n = 100 tubules from 3 kidneys per condition. $^{***}P$=0.0002, $^{\#}P$<0.0001.
Bars indicate mean ± SEM. One-way ANOVA followed by Tukey's post-hoc test.

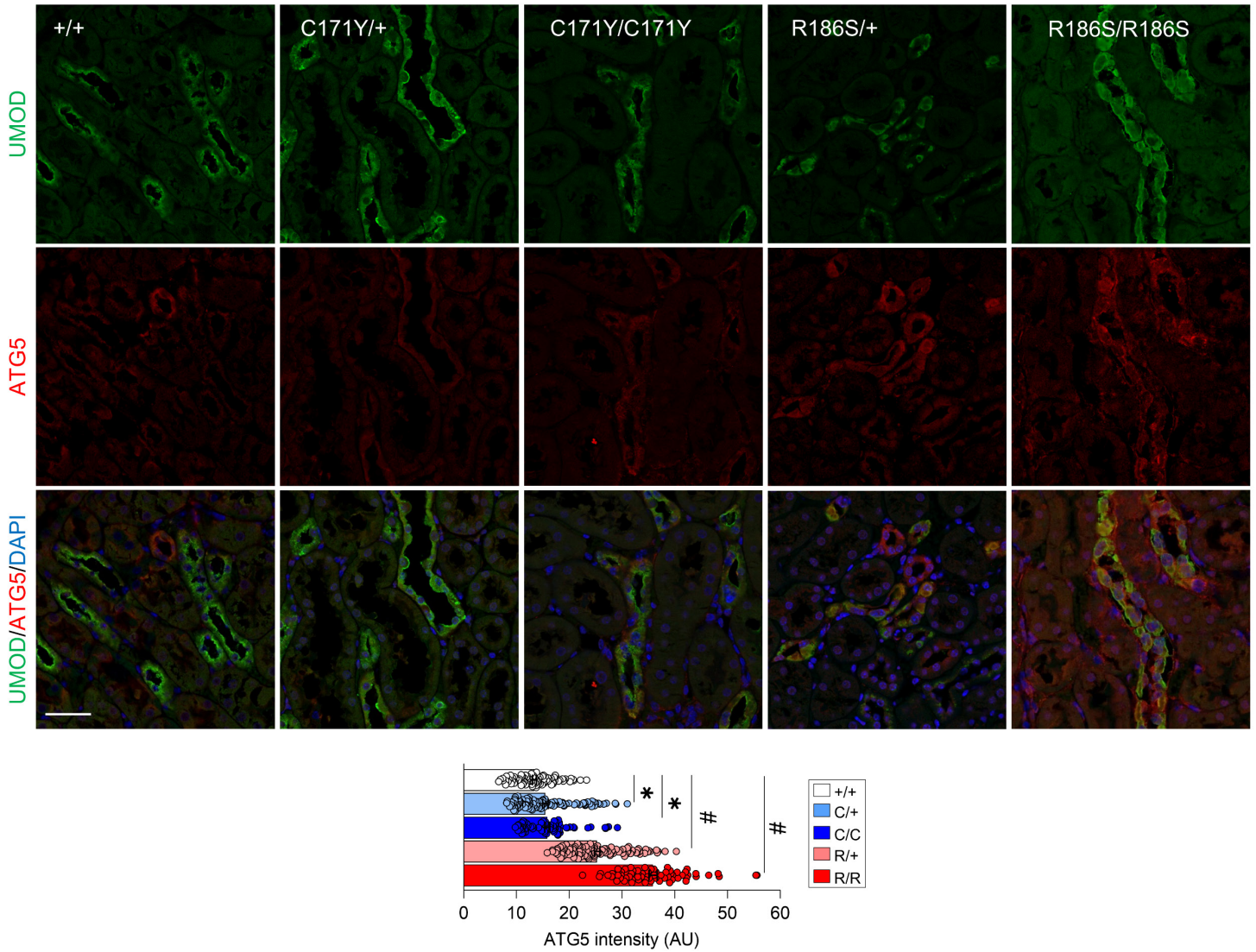

Appendix Figure S6: Markers of autophagy induction in *Umod* KI mouse kidneys.

Representative immunofluorescence analysis of UMOD (green) and ATG5 (red) on kidney sections from 4-month-old *Umod* KI mice. Nuclei are counterstained with DAPI (blue). Scale bar: 25 µm, n ≥ 67 tubules from 3 kidneys per condition. Bars indicate mean ± SEM. One-way ANOVA followed by Tukey's post-hoc test, $^{*}P$(+/+ vs. C/+)=0.032, $^{*}P$(+/+ vs. C/C)=0.0153, $^{\#}P$<0.0001.

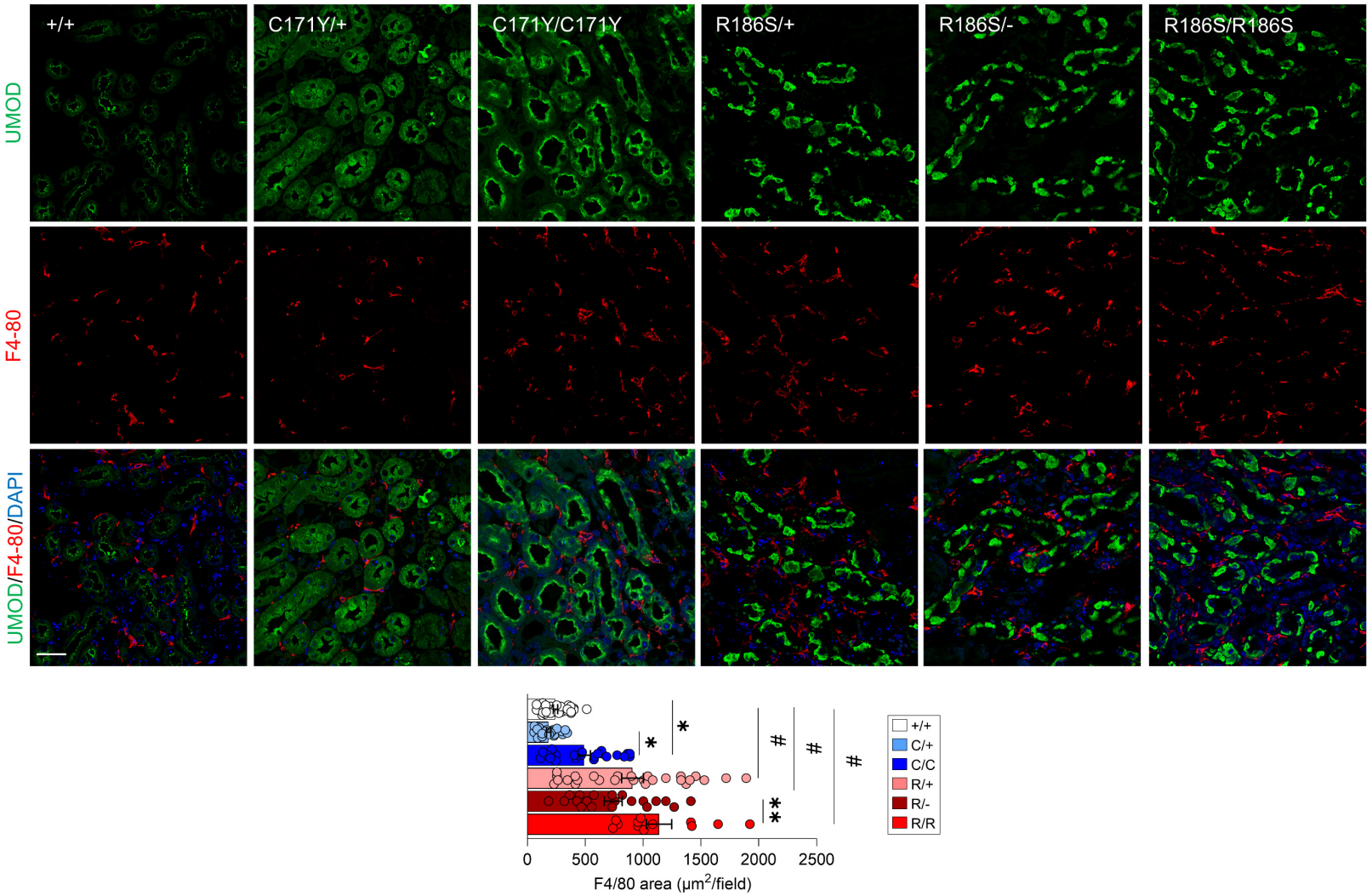

Appendix Figure S7: Macrophage infiltration in *Umod* KI mouse kidneys.

Confocal analysis of kidney sections from 4-month mice stained with anti-uromodulin (green) and anti-F4-80 (red). n ≥12 fields from 3 kidneys per condition. Nuclei are stained with DAPI (blue). Scale bar: 25 µm. Bars indicate the mean ± SEM. One-way ANOVA with Tukey's post hoc test, $^{*}P$(+/+ vs. C/C)=0.0342, $^{*}P$(C/+ vs. C/C)=0.0103, $^{**}P$=0.0059, $^{\#}P$<0.0001.

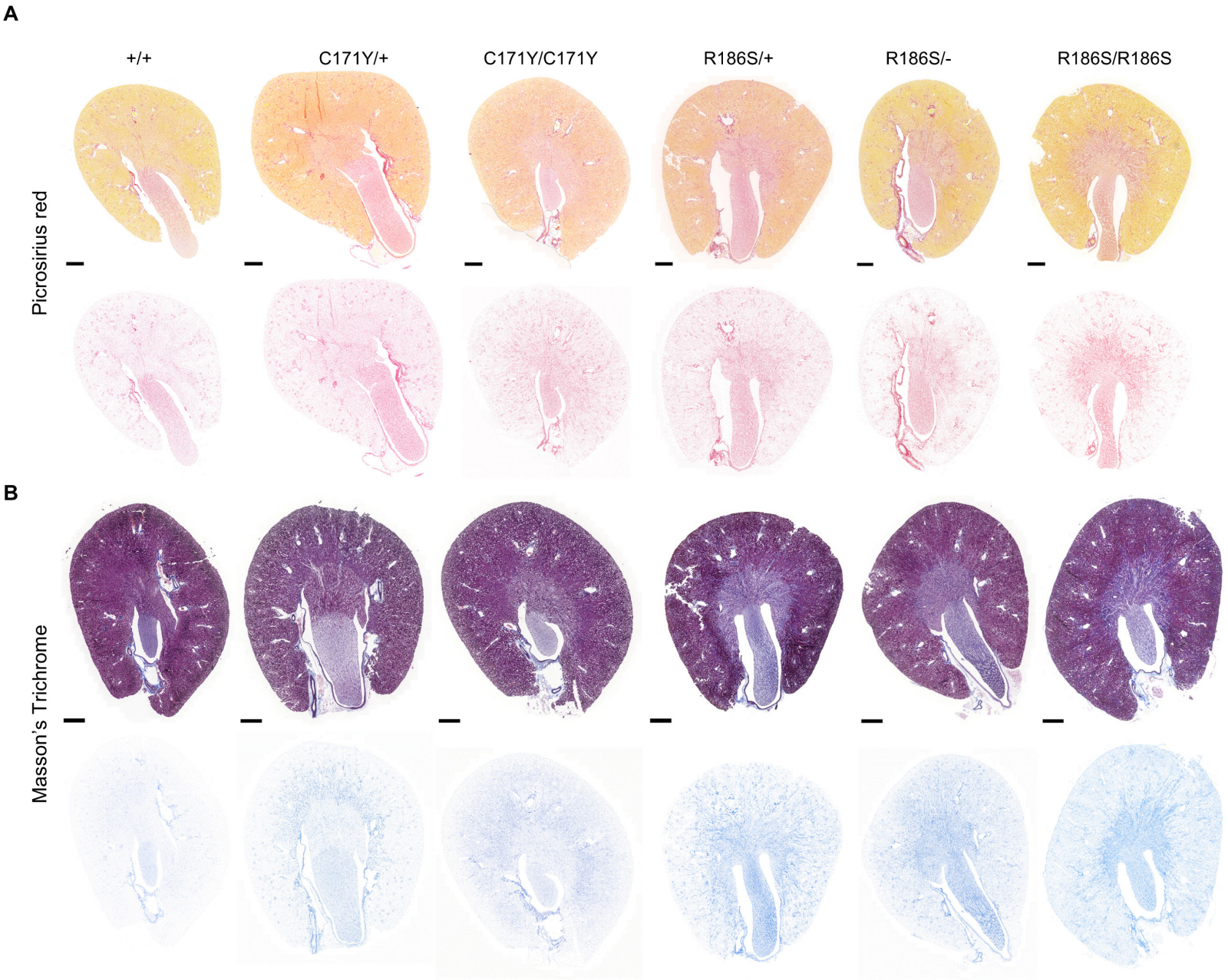
A
+/+
C171Y/+
C171Y/C171Y
R186S/+
R186S/-
R186S/R186S
Picrosirius red
B
Masson's Trichrome

Appendix Figure S8: Characterization of interstitial fibrosis in *Umod* KI mouse kidneys.

(**A**-**B**) Representative Picrosirius red (**A**) and Masson's Trichrome (**B**) stainings on kidney sections from 4-month-old *Umod* KI mice (n=3 to 11 animals per group). Deconvoluted collagen signal is shown below each image. Scale bars: 100 µm

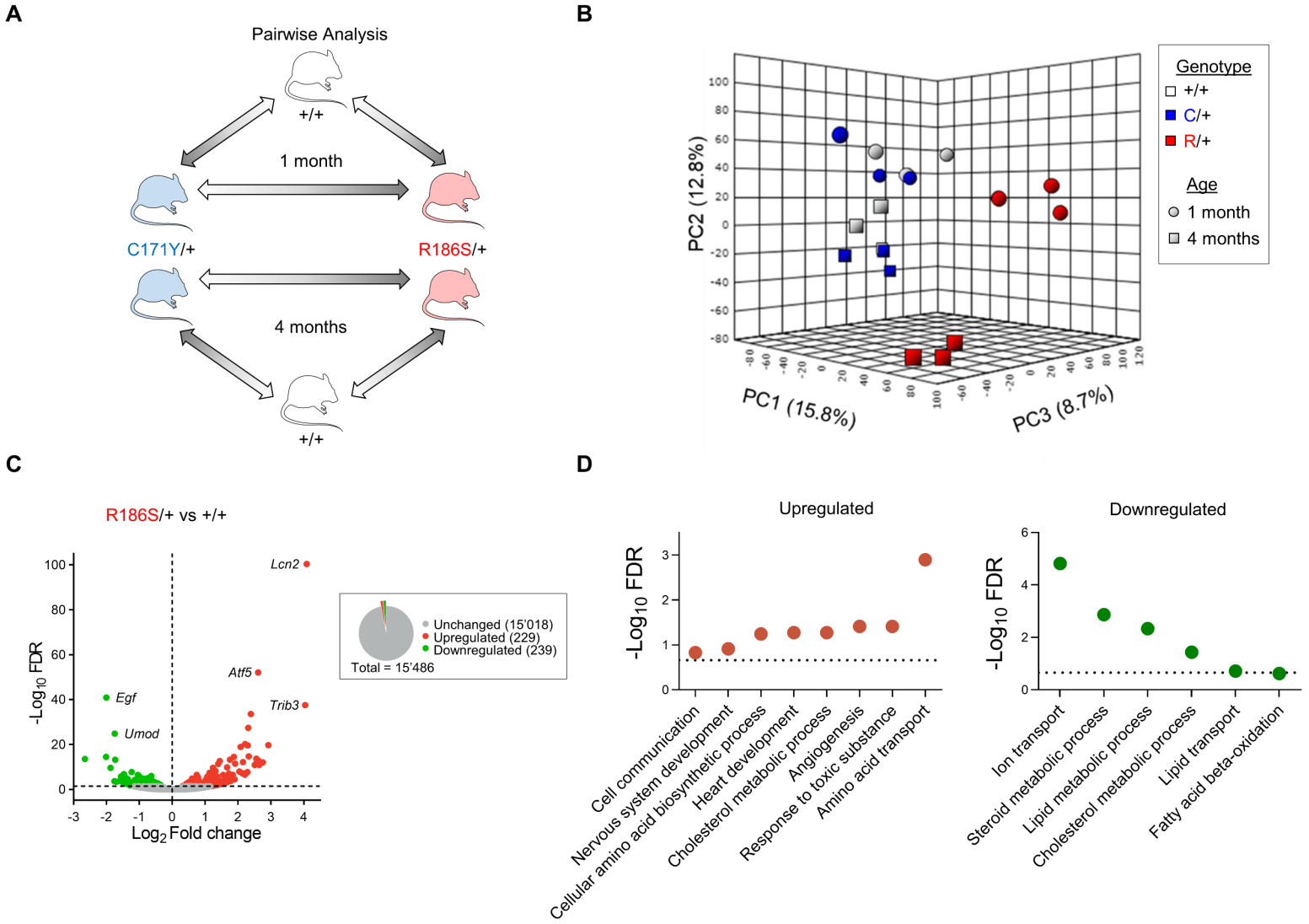

Appendix Figure S9: RNA-seq analyses in 1-month-old R186S/+ kidneys.

(**A**) Experimental design for RNA-Seq on whole kidney lysates from 1 and 4 months male *Umod* KI mice.
(**B**) Principal component analysis (PCA) of RNA-Seq data of kidneys from 1-month-old and 4-month-old *Umod* KI mice.
(**C**) Volcano plot showing differently expressed genes (DEGs) between R186S/+ and +/+ 1-month-old kidneys. Genes not significantly changed (FDR > 0.05) are shown in grey, whereas genes that are up- or downregulated in R186S/+ are shown in red and green respectively. The total number of unchanged, up- and downregulated genes are summarized in the pie chart.
(**D**) Over-representation analysis showing up- (red) and downregulated (green) biological processes of gene ontology in 1-month-old R186S/+ kidneys.

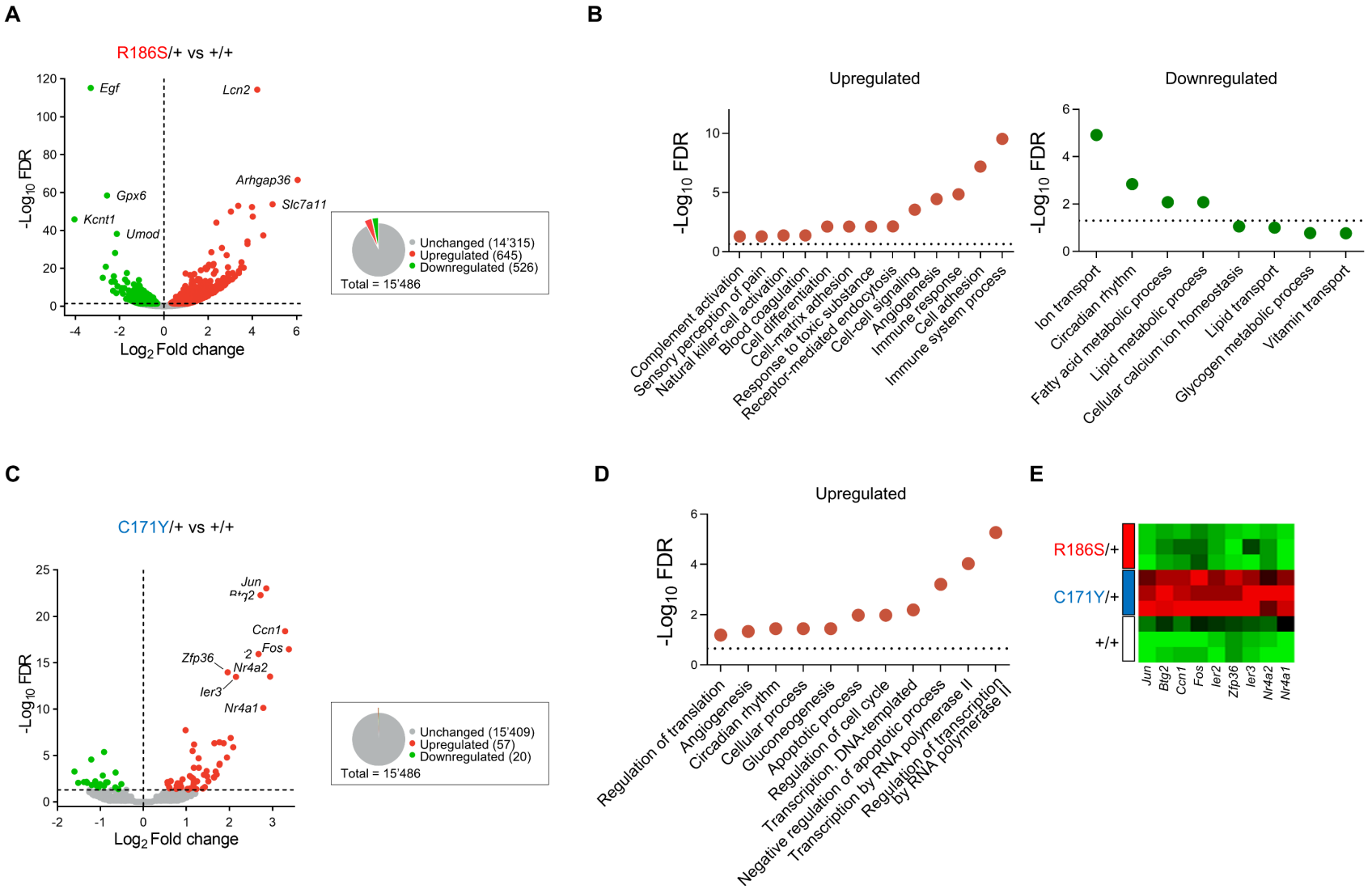

Appendix Figure S10: Differential expression and affected pathways in 4-month-old *Umod* KI kidneys.

(**A**) Volcano plot showing differently expressed genes (DEGs) between +/+ and R186S/+ kidneys at 4 months.

(**B**) Over-representation analysis (ORA) showing up- and downregulated biological processes in 4-months-old R186S/+ kidneys.

(**C**) Volcano plot showing DEGs between C171Y/+ and +/+ kidneys at 4 months. Genes not significantly changed (FDR > 0.05) are shown in grey, whereas genes that are up- or downregulated in *Umod* KI are shown in red and green respectively. The total number of unchanged, up- and downregulated genes are summarized in the pie chart.

(**D**) ORA showing upregulated biological processes in 4-month-old C171Y/+ kidneys. No significantly downregulated pathways were identified. (**e**) Heatmap of transcriptional regulation genes upregulated in 4-month-old C171Y/+ kidneys.

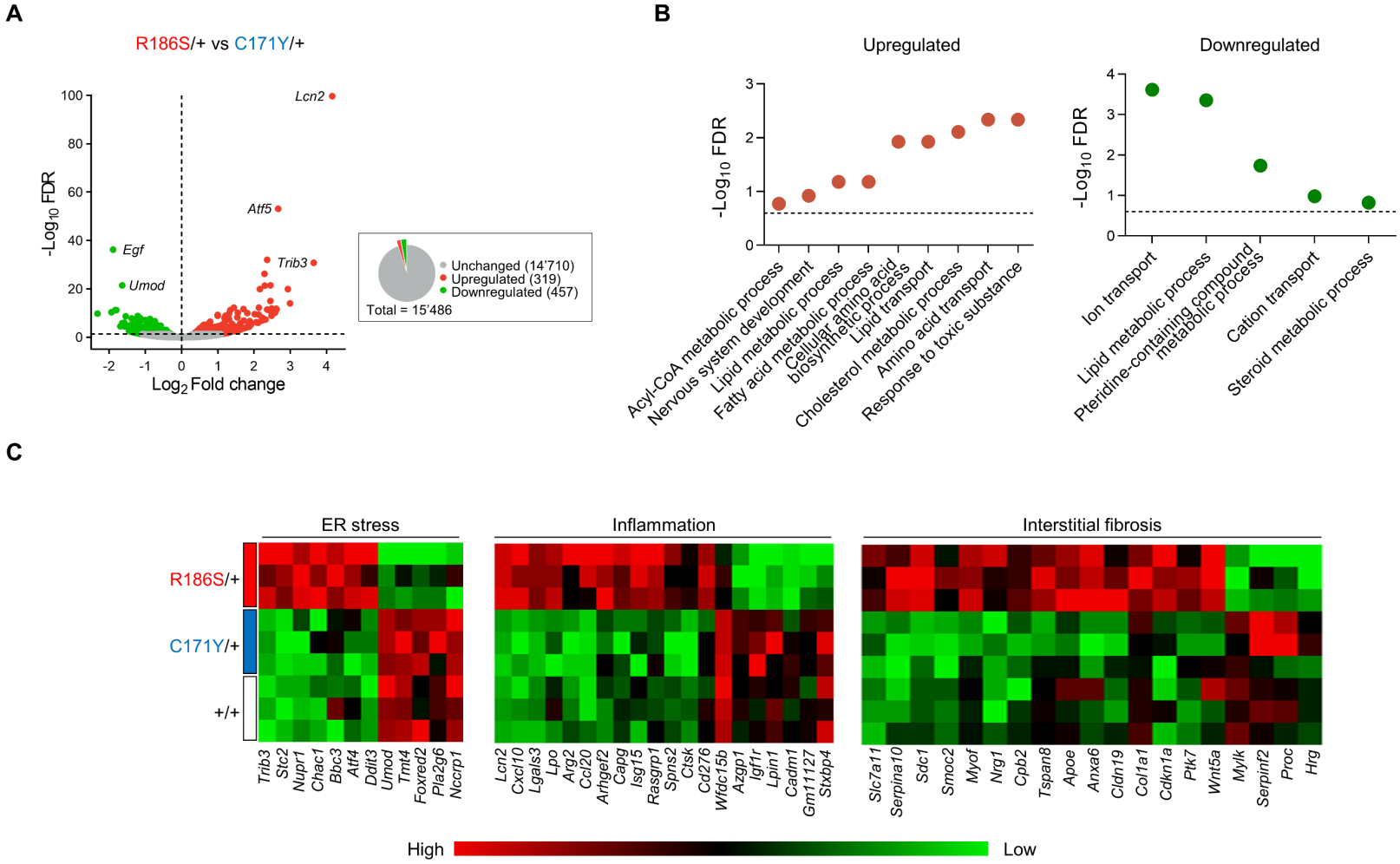

Appendix Figure S11: Disease progression signature in *Umod* KI kidneys.

(**A**) Volcano plot showing differently expressed genes (DEGs) between R186S/+ and C171Y/+ kidneys at 1 month. Genes not significantly changed (FDR > 0.05) are shown in grey, whereas genes that are up- or downregulated in R186S/+ are shown in red and green respectively. The total number of unchanged, up- and downregulated genes are summarized in the pie chart.
(**B**) Over-representation analysis (ORA) showing up- (red) and downregulated (green) biological processes in 1-month-old R186S/+ kidneys compared to C171Y/+.
(**C**) Heat map of selected pathways involved in the disease progression of *Umod* KI mice at 1 month. R186S/+ kidneys showed upregulation of ER stress (*Atf4*, *Ddit3*, *Nupr1*, *Trib3*), increased expression of genes associated with inflammation (*Lcn2*, *Lgals3*) and fibrosis (*Serpina10*, *Col1a1*), whereas C171Y/+ kidneys were virtually indistinguishable from +/+.

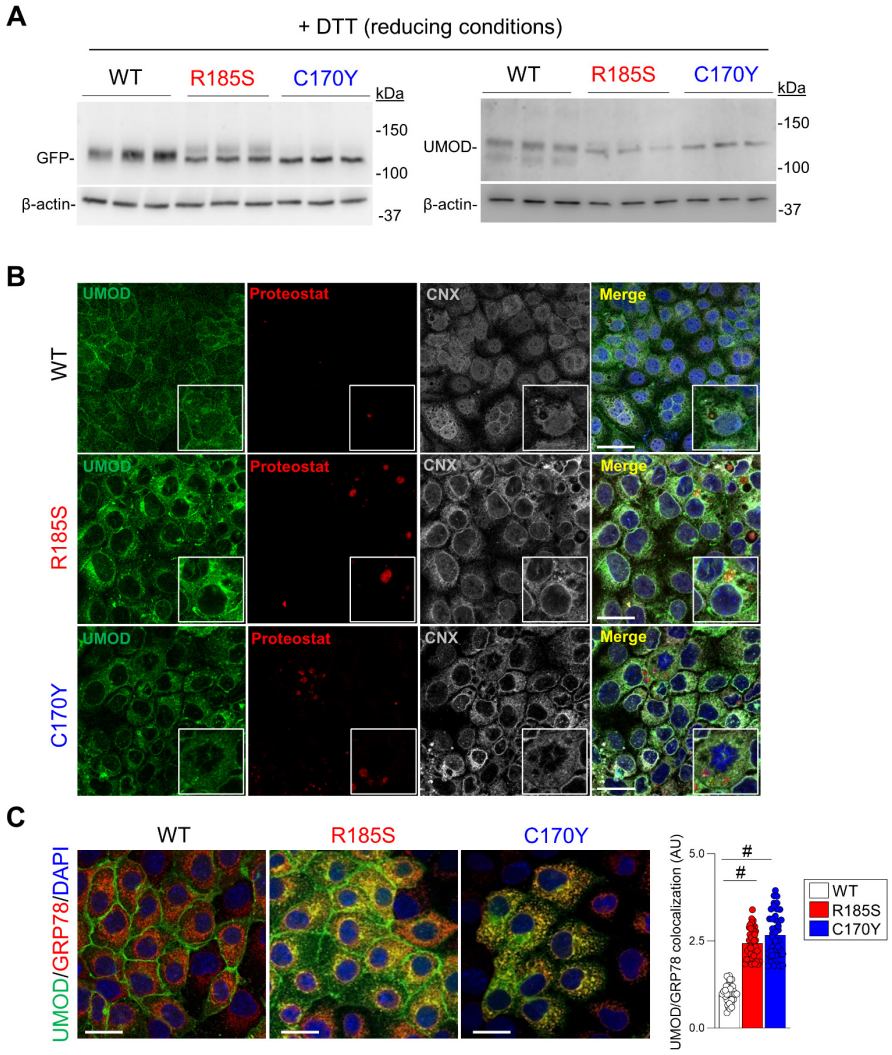
A
+ DTT (reducing conditions)
WT
R185S
C170Y
kDa
GFP-
-150
-100
β-actin-
-37
UMOD-
B
UMOD
Proteostat
CNX
Merge
C
UMOD/GRP78/DAPI
UMOD/GRP78 colocalization (AU)
5.0
2.5
0.0
#
WT
R185S
C170Y
D
+
IGG
IB: UMOD-
IP: GRP78-
-75
E
Hspa5 (GRP78)
Xbp1s
Lcn2
Atf4
Ddit3 (CHOP)
Eif2a
Eif2ak3 (PERK)
Fold change (relative to WT)
F
Rtn3
Ccpg1
Sec62
Retreg1
Sec61a1
Hsp90ab1
Dnajb4
Dnaja4

Appendix Figure S12: Distinct UMOD mutations trigger differential ER quality control responses.

(**A**) Immunoblot analysis of GFP and UMOD in lysates from *UMOD-GFP* cells. Samples were run in reducing conditions. β-actin used as a loading control.
(**B**) Immunofluorescence analysis of UMOD (green), Proteostat (red) and CNX (gray) in *UMOD-GFP* cells. Scale bar: 30 μm.
(**C**) Immunofluorescence analysis of UMOD (green) and GRP78/BiP (red) in *UMOD-GFP* cells. Co-localization is expressed as arbitrary units (AU). Scale bar: 30 μm (n=33 to 44 cells per group), $^{\#}P<0.0001$.
(**D**) Co-immunoprecipitation experiments in *UMOD-GFP* cells showing interaction between UMOD and GRP78/BiP.
(**E**) RT-qPCR analysis of unfolded protein response (UPR) effectors in in *UMOD-GFP* cells. Values are expressed as relative to WT (black dotted line, n = 6 biological replicates). *Hspa5*: $^{***}P$(WT vs. C170Y)=0.0008; *Xbp1s:* $^{\#}P$(WT vs. C170Y)<0.0001, $^{\dagger\dagger}P$(C170Y vs. R185S)=0.0018, $^{**}P$(WT vs. R185S)=0.0045; *Lcn2*: $^{\#}P$(WT vs. R185S)<0.0001, $^{\dagger\dagger\dagger\dagger}P$(C170Y vs. R185S)<0.0001; *Ddit3:* $^{**}P$(WT vs. R185S)=0.0083, $^{\dagger\dagger}P$(WT vs. C170Y)=0.0019, *Eif2a:* $^{*}P$(WT vs. R185S)=0.0118.
(**F**) RT-qPCR analysis of protein folding/degradation genes in *UMOD-GFP* cells. Values are expressed as relative to WT (black dotted line) (n =4 to 6 biological replicates). *Rtn3:* $^{**}P$(WT vs. C170Y)=0.002, $^{\dagger\dagger}P$=0.0028 (C170Y vs. R185S); *Ccpg1:* $^{**}P$(WT vs. C170Y)=0.0078, $^{\dagger\dagger\dagger\dagger}P$(C170Y vs. R185S)<0.0001, $^{**}P$(WT vs. R185S)=0.0023; *Sec62*: $^{***}P$(WT vs. C170Y)=0.0008, $^{\dagger\dagger\dagger}P$(C170Y vs. R185S)=0.0002; *Retreg1:* $^{**}P$(WT vs. C170Y)=0.002, $^{\dagger}P$(R185S vs. C170Y)=0.017; *Sec61a1:* $^{***}P$(WT vs. C170Y)=0.0005, $^{**}P$(WT vs. R185S)=0.0013; *Dnaja4:* $^{*}P$(WT vs. C170Y)=0.0209.
Bars indicate mean ± SEM. One-way ANOVA followed by Tukey's post-hoc test.

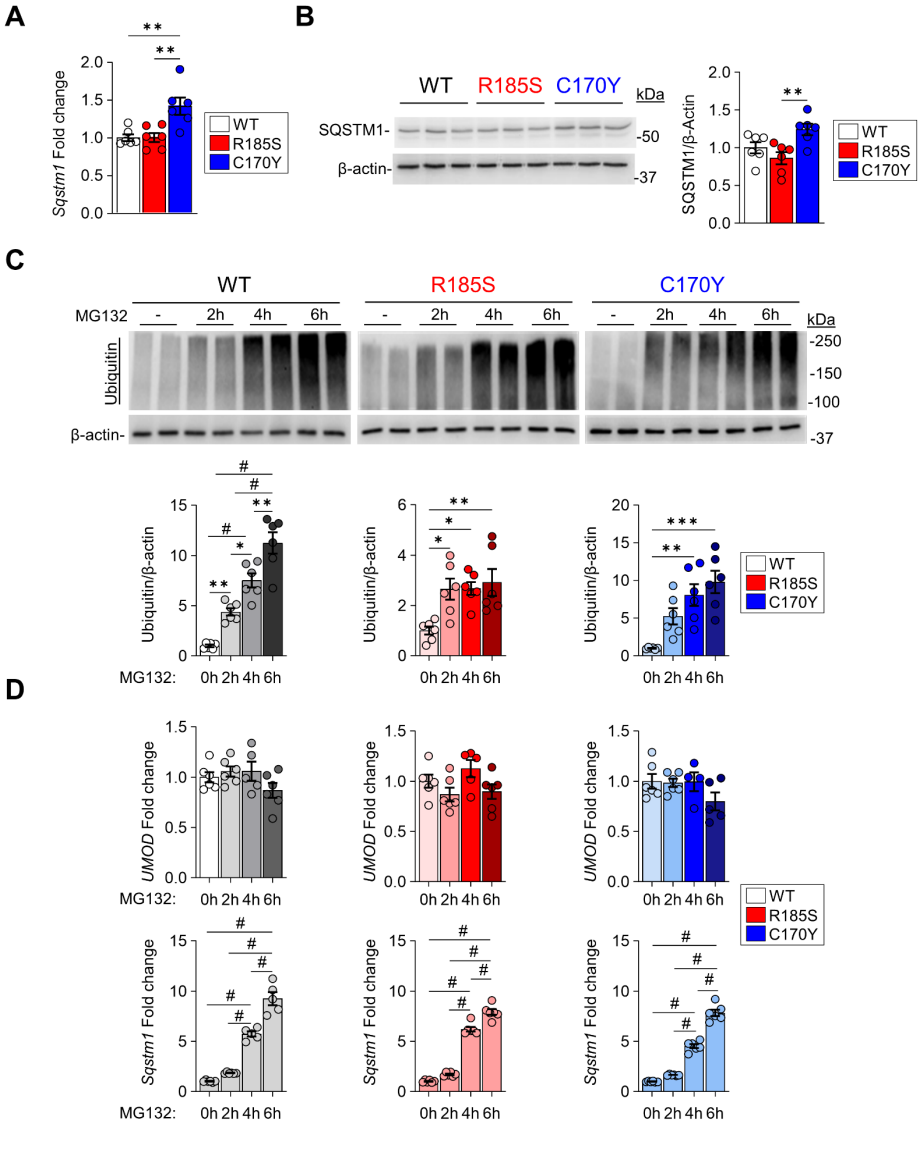
A
B
C
D
E
F
WT
R185S
C170Y
Sqstm1 Fold change
SQSTM1-
β-actin-
kDa
SQSTM1/β-Actin
MG132
Ubiquitin
Ubiquitin/β-actin
UMOD Fold change
Sqstm1 Fold change
DMSO
MG132
UMOD/SQSTM1/DAPI
SQSTM1 Intensity (AU)
UMOD WT
UMOD R185S
UMOD C170Y
Bortezomib:
UMOD-
Fold change

Appendix Figure S13: Proteasomal inhibition induces mutant UMOD accumulation.

(**A**) RT-qPCR analysis of *Sqstm1* gene in *UMOD-GFP* cells. Values are expressed as relative to WT cells (n=6 biological replicates), $^{**}P$(R185S vs. C170Y)=0.0058, $^{**}P$(WT vs. C170Y)=0.0056.
(**B**) Immunoblot analysis of SQSTM1 in *UMOD-GFP* cells. β-actin used as a loading control. Densitometry analysis relative to WT cells (n=6 biological replicates), $^{**}P$=0.0084.
(**C**) Immunoblot analysis of ubiquitin in *UMOD-GFP* cell lysates following MG123 time course. Densitometry analysis relative to untreated cells (n = 6 biological replicates). WT: $^{**}P$(0h vs. 2h)=0.0096, $^{*}P$=0.0177, $^{**}P$(4h vs. 6h)= 0.0041; R185S: $^{*}P$(0h vs. 2h)=0.0177, $^{*}P$(0h vs. 4h)=0.0216, $^{**}P$=0.0079; C170Y: $^{**}P$=0.002, $^{***}P$=0.0002.
(**D**) RT-qPCR analysis of *UMOD* and *Sqstm1* genes in *UMOD-GFP* cells following time-dependent MG132 treatment. Values are relative to untreated (0h) cells (n ≥4 biological replicates), $^{\#}P$<0.0001.
(**E**) Representative immunofluorescence of UMOD (green) and SQSTM1 (red) in *UMOD-GFP* cells. Nuclei counterstained with DAPI (blue). Scale bar: 15 μm (n = 30 cells per group), $^{\#}P$<0.0001.
(**F**) Immunoblot analysis of ubiquitin, UMOD in *UMOD-GFP* cell lysates following Bortezomib time-course. β-actin used as a loading control. Densitometry analysis relative to fed cells (n ≥4 biological replicates). WT, Ubiquitin: $^{**}P$(0h vs. 4h)=0.0013, $^{**}P$(0h vs. 6h)=0.0011, $^{*}P$(2h vs. 4h)=0.0322, $^{*}P$(4h vs. 6h)=0.0267; R185S, Ubiquitin: $^{**}P$(0h vs. 4h)=0.0013, $^{**}P$(2h vs. 6h)=0.0022; C170Y, UMOD: $^{**}P$(0h vs. 6h)=0.0045, $^{**}P$(4h vs. 6h)=0.0051; Ubiquitin: $^{*}P$(0h vs. 2h)=0.0429, $^{**}P$=0.0014, $^{***}P$=0.0002, $^{*}P$(2h vs. 6h)=0.031; $^{\#}P$ <0.0001.
Bars indicate mean ± SEM. One-way ANOVA followed by Tukey's post-hoc test.

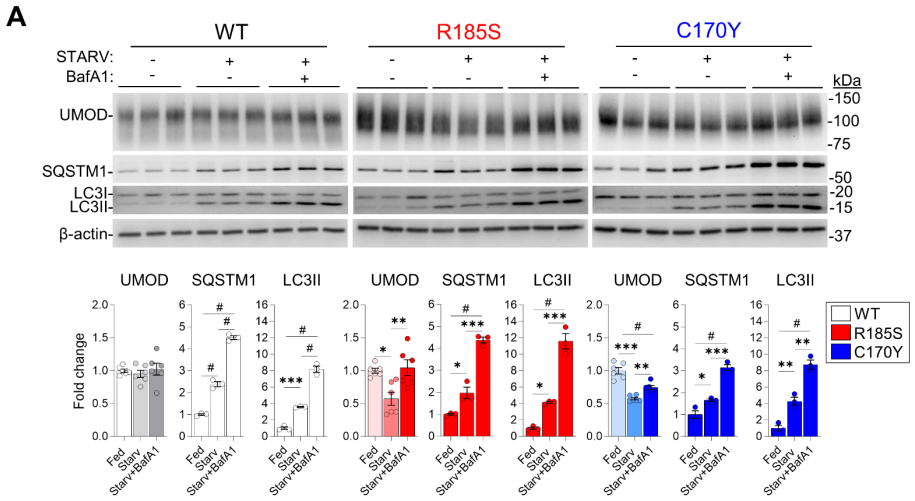
A
WT
R185S
C170Y
STARV:
BafA1:
kDa
UMOD-
SQSTM1-
LC3I-
LC3II-
β-actin-
-150
-100
-75
-50
-20
-15
-37
UMOD
SQSTM1
LC3II
Fold change
Fed
Starv
Starv+BafA1
WT
R185S
C170Y

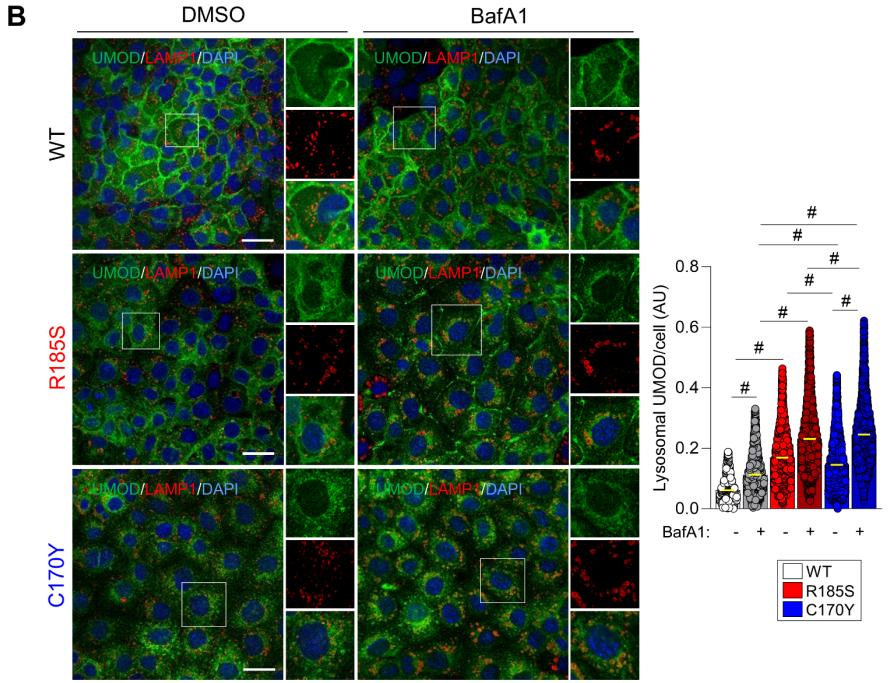
B
DMSO
BafA1
WT
R185S
C170Y
UMOD/LAMP1/DAPI
Lysosomal UMOD/cell (AU)
BafA1:
WT
R185S
C170Y

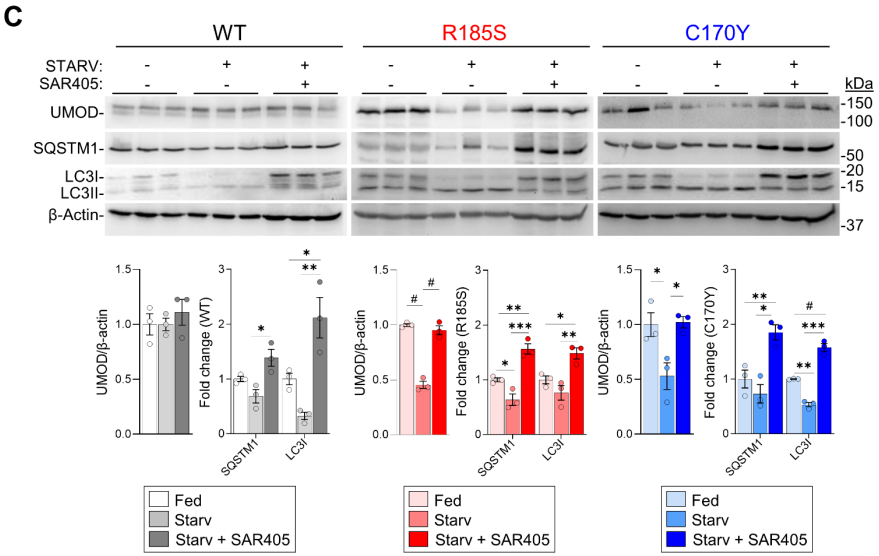
C
WT
R185S
C170Y
STARV:
SAR405:
kDa
UMOD-
SQSTM1-
LC3I-
LC3II-
β-Actin-
-150
-100
-50
-20
-15
-37
UMOD/β-actin
Fold change (WT)
Fold change (R185S)
Fold change (C170Y)
SQSTM1
LC3I
Fed
Starv
Starv + SAR405

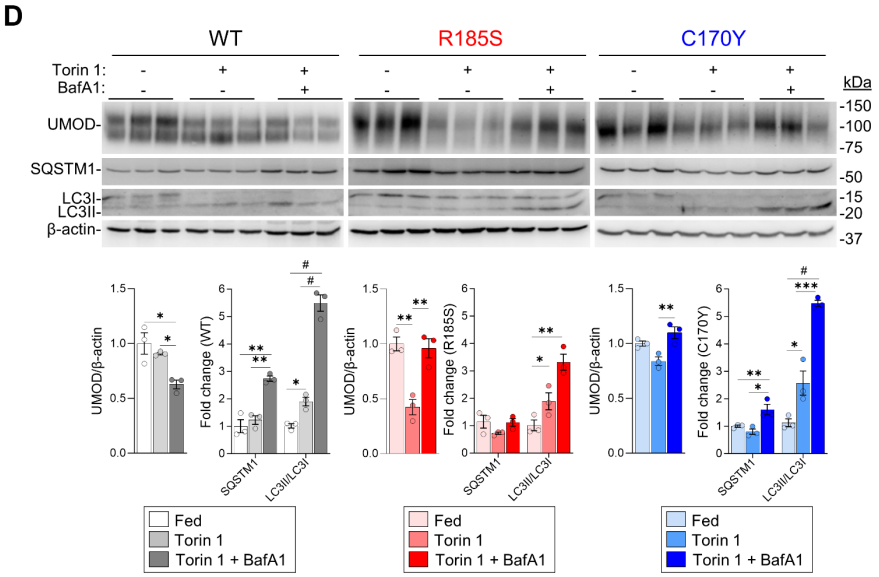
D
WT
R185S
C170Y
Torin 1:
BafA1:
kDa
UMOD-
SQSTM1-
LC3I-
LC3II-
β-actin-
-150
-100
-75
-50
-15
-20
-37
UMOD/β-actin
Fold change (WT)
Fold change (R185S)
Fold change (C170Y)
SQSTM1
LC3II/LC3I
Fed
Torin 1
Torin 1 + BafA1

Appendix Figure S14: Autophagy modulation impacts on mutant UMOD levels.

(**A**) Immunoblot analysis of UMOD, SQSTM1 and LC3 in *UMOD-GFP* cell lysates following starvation and Bafilomycin A1 treatment. β-actin used as a loading control. Densitometry analysis relative to fed (n=3 biological replicates), WT, LC3II: $^{***}P$=0.0007; R185S, UMOD: $^{*}P$=0.0136,$^{**}P$=0.0067; SQSTM1: $^{*}P$=0.0175, $^{***}P$=0.0002; LC3II: $^{*}P$=0.0164, $^{***}P$=0.0002; C170Y, UMOD: $^{***}P$=0.0003,$^{**}P$ = 0.0096; SQSTM1: $^{*}P$=0.0282, $^{***}P$=0.0004; LC3II: $^{**}P$(Fed vs. Starv)=0.006, $^{**}P$(Starv vs. Starv+ BafA1)=0.0013; $^{\#}P$<0.0001.
(**B**) Representative immunofluorescence of UMOD (green) and LAMP1 (red) in *UMOD-GFP* cells following BafA1 treatment. Nuclei counterstained with DAPI (blue). Scale bar: 15 μm (n ≥ 20 cells/field, 5 fields per condition), $^{\#}P$<0.0001.
(**C**) Immunoblot analysis of UMOD, SQSTM1 and LC3 in *UMOD-GFP* cell lysates following SAR405 treatment. Densitometry analysis relative to fed (n=3 biological replicates). WT, SQSTM1: $^{*}P$=0.0129; LC3I: $^{**}P$=0.0033, $^{*}P$=0.0296; R185S, SQSTM1: $^{*}P$=0.0486, $^{**}P$=0.0073, $^{***}P$=0.0005; LC3I: $^{**}P$=0.0070, $^{*}P$=0.0410; C170Y, UMOD: $^{*}P$(Fed vs. Starv)=0.0342, $^{*}P$(Starv vs. Starv + SAR405)=0.0283; SQSTM1: $^{**}P$=0.055, $^{*}P$=0.0198; LC3I: $^{**}P$=0.0011, $^{***}P$=0.0004; $^{\#}P$<0.0001.
(**D**) Immunoblot analysis of UMOD, SQSTM1 and LC3 in *UMOD-GFP* cell lysates following Torin 1 and BafA1 treatment. Densitometry analysis relative to fed cells (n=3 biological replicates). WT, UMOD: $^{*}P$(Fed vs. Torin 1)=0.0118, $^{*}P$(Torin 1 vs. Torin 1+BafA1)=0.0399; SQSTM1: $^{**}P$(Fed vs. Torin 1+BafA1)=0.001, $^{**}P$(Torin 1 vs. Torin 1+BafA1)=0.0022; LC3II/I: $^{*}P$=0.0476; R185S, UMOD: $^{**}P$(Fed vs. Torin 1)=0.0035, $^{**}P$(Torin 1 vs. Torin 1+BafA1)=0.005; LC3II/I: $^{*}P$=0.023, $^{**}P$=0.0023; C170Y, UMOD: $^{**}P$=0.0096; SQSTM1: $^{*}P$=0.0336, $^{**}P$=0.0094; LC3II/I: $^{*}P$=0.0229, $^{***}P$=0.0007; $^{\#}P$< 0.0001.
Bars indicate mean ± SEM. One-way ANOVA followed by Tukey's post-hoc test.

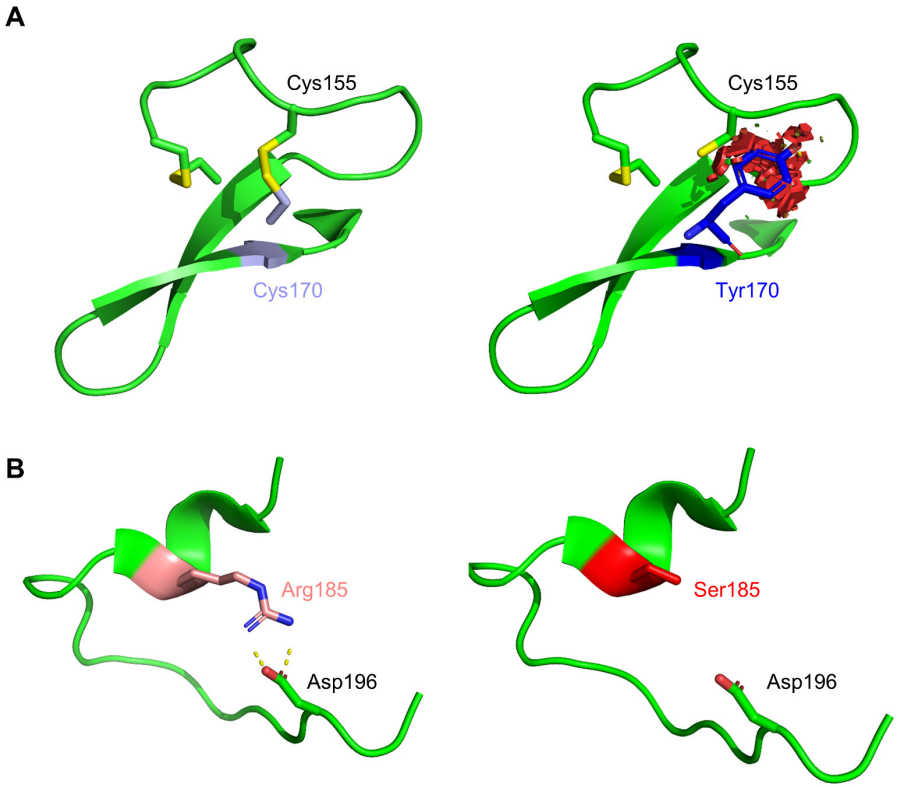

Appendix Figure S15: Structural modelling of UMOD mutations

(**A**, **B**) Modeling of the UMOD p.Cys170Tyr (**A**) and p.Arg185Ser (**B**) mutants. Clashes in the structure are represented by red dots and are visible only in the p.Cys170Tyr mutant. Models were generated with PyMOL (Schrödinger LLC).

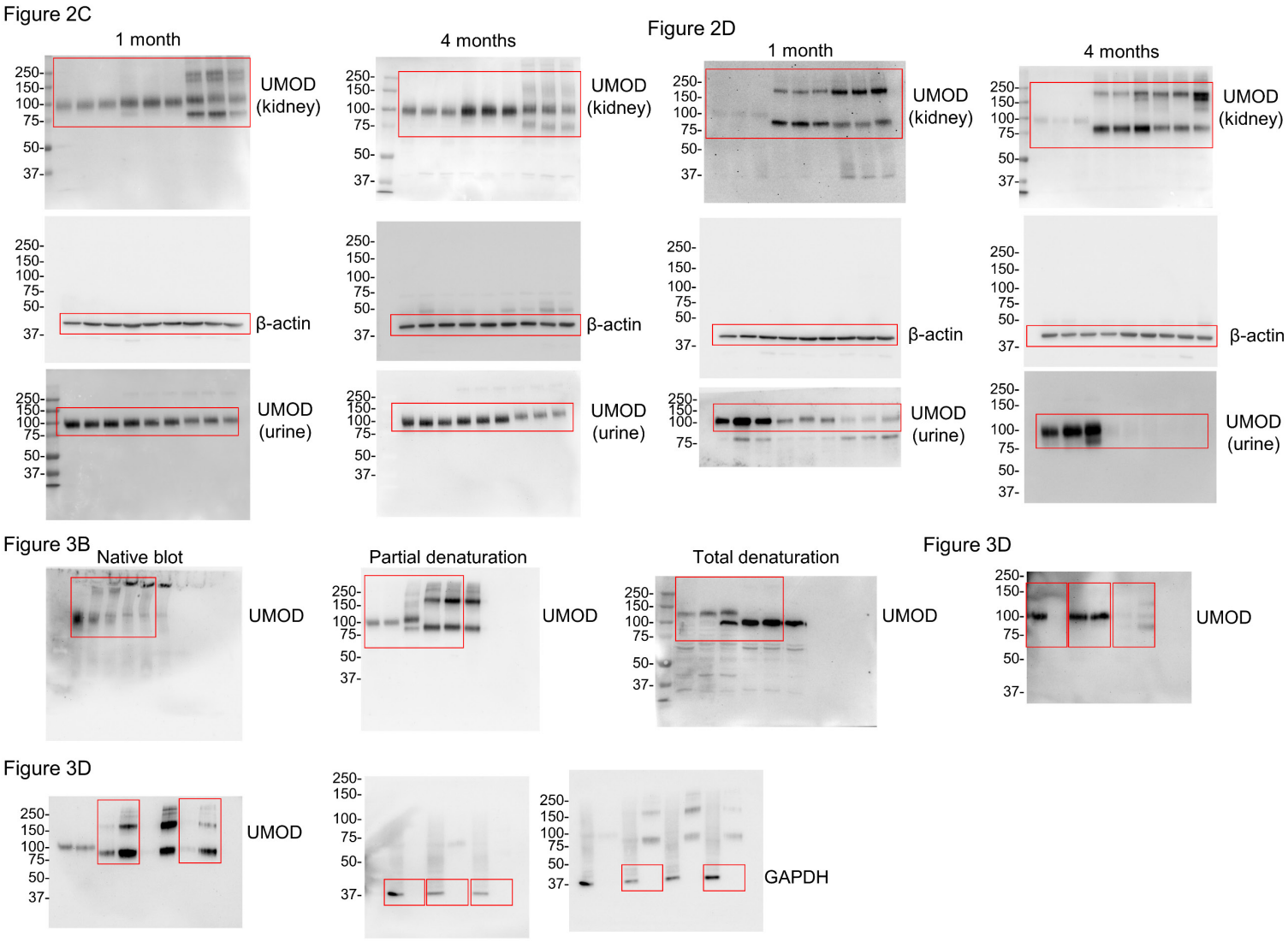

Appendix Figure S16: Uncropped Western blot membranes.

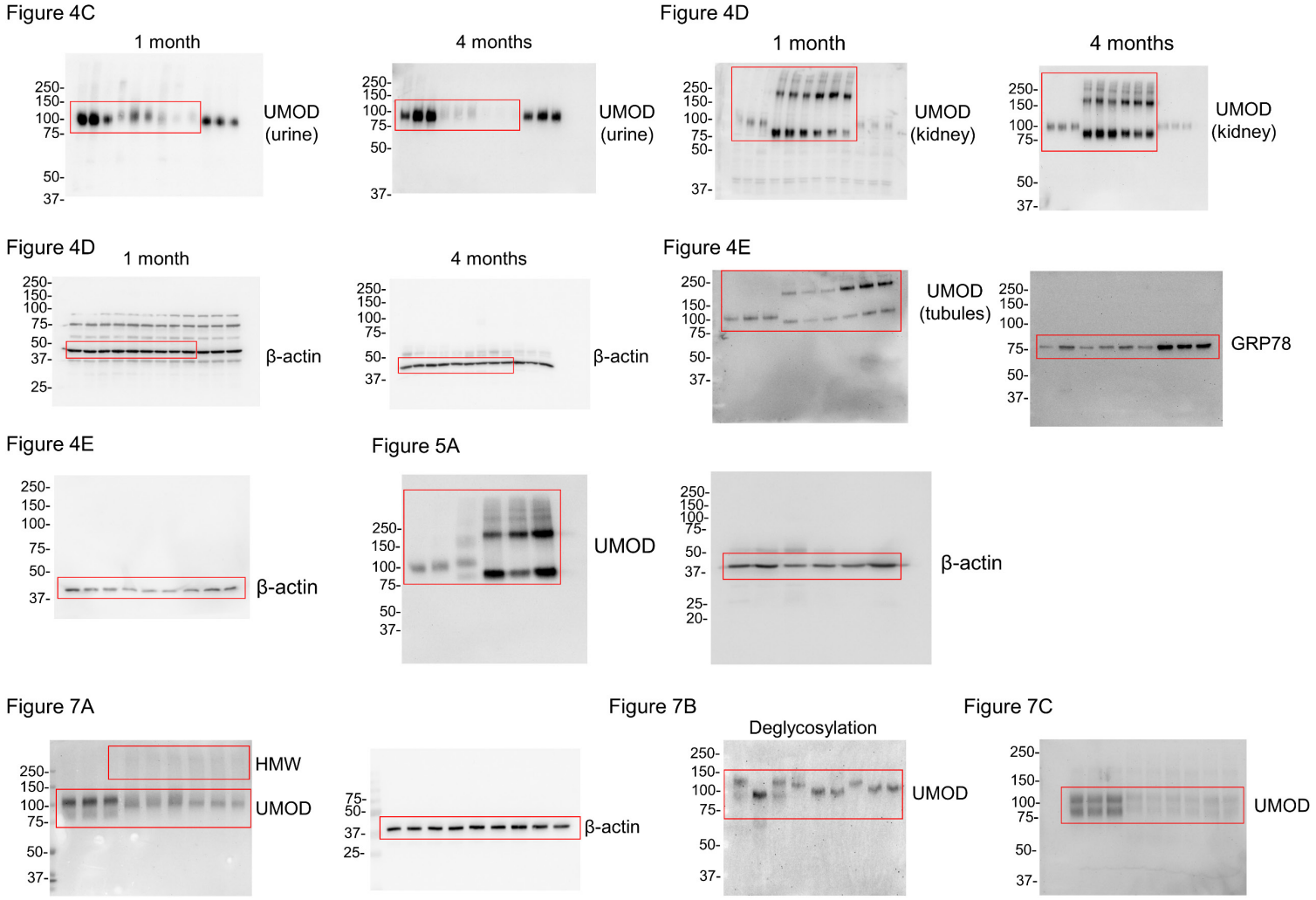

Appendix Figure S16 (continued).

Figure 7G

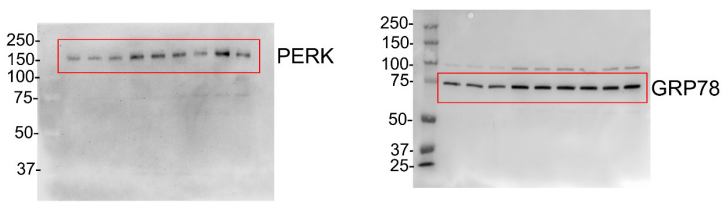

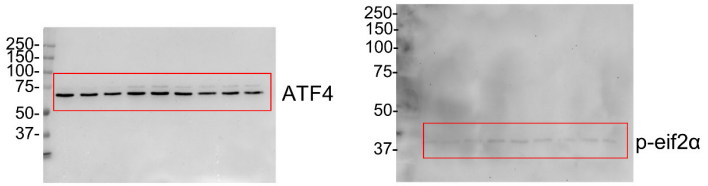

Figure 7G

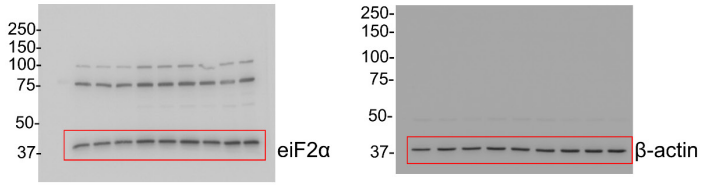

Figure 8B

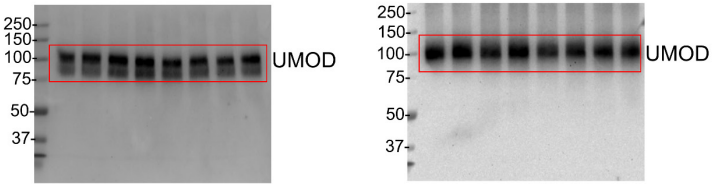

Figure 8B

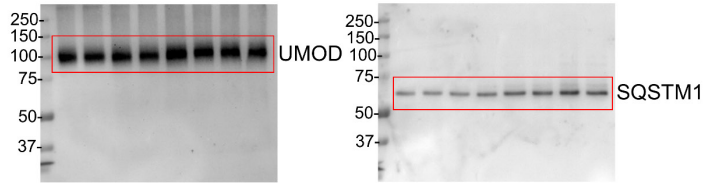

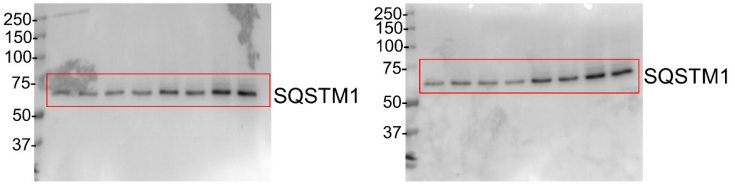

Figure 8B

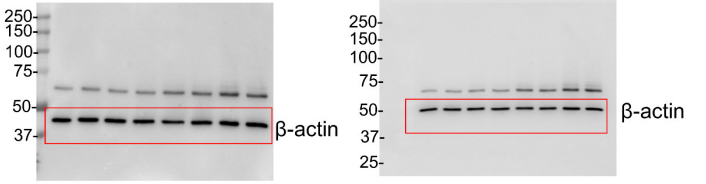

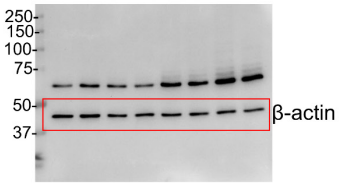

Appendix Figure 16 (continued).

Figure 8D

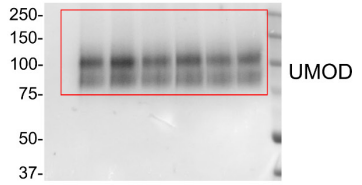

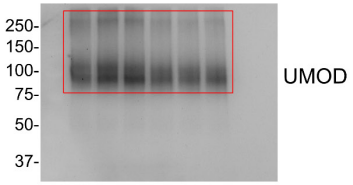

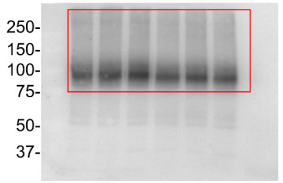

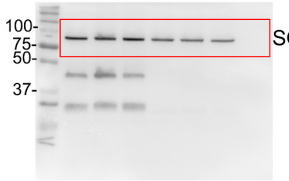

Figure 8D

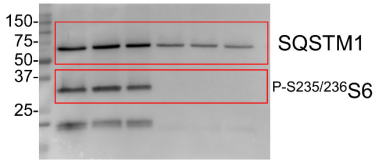

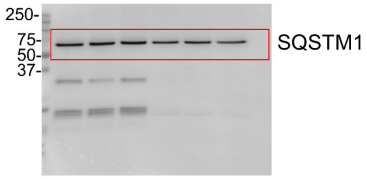

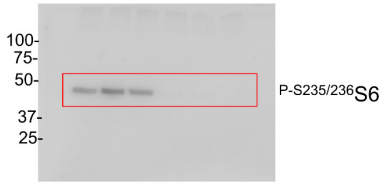

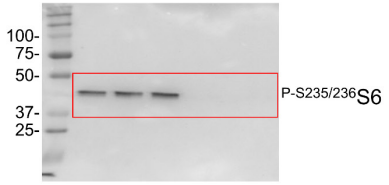

Figure 8D

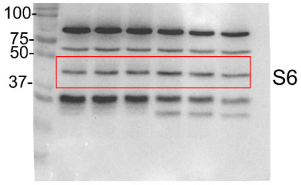

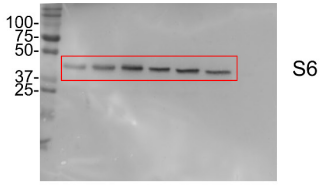

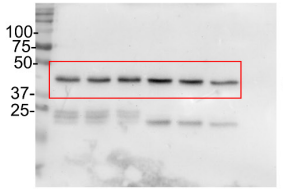

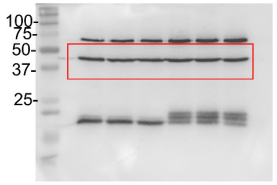

Figure 8D

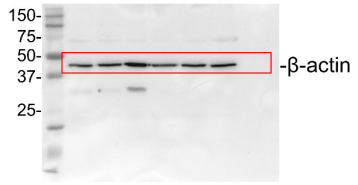

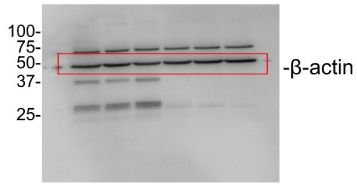

Appendix Figure 16 (continued).

Appendix Table S1: Clinical characteristics of p. (Arg185Ser) ADTKD-UMOD family.

	Gender	CKD (age)	Kidney failure (age)	Hyperuricemia (age)	Gout (age)
p.R185S III.1	F	Y	Y (NA)	Y	Y (40y)
p.R185S III.2	F	Y	Y (50y)	NA	NA
p.R185S IV.1	M	Y	Y (43y)	Y	Y
p.R185S IV.2	M	Y (32y)	Y (36y)	Y	Y (32y)
p.R185S IV.3	M	Y (19y)	Y (28y)	Y	Y (9y)
p.R185S IV.4	F	Y	N (41y)	Y (34y)	N
p.R185S IV.5	F	Y	Y (38y)	Y	Y (18y)
p.R185S IV.6	M	Y (38y)	Y (42y)	Y	Y (26y)
p.R185S V.1	M	Y	N (24y)	NA	NA
p.R185S V.2	M	Y	N (34y)	Y	Y (25y)

M, male; F, female; Y, yes; N, no; NA, not available; CKD, chronic kidney disease; eGFR, estimated glomerular filtration rate.

Appendix Table S2: Clinical characteristics of p. (Cys170Tyr) ADTKD-*UMOD* families.

F1	Gender	CKD (age)	Kidney failure (age)	Hyperuricemia	Gout (age)
p.C170Y I.1	M	Y	Y (63y)	Y	Y
p.C170Y II.1	M	Y (41y)	Y (58y; post-nephrectomy)*	Y	Y (55y)
p.C170Y III.1	F	Y (43y)	N	Y	N
p.C170Y III.2	F	Y	N (28y)	NA	NA
p.C170Y IV.1	F	N (12y)	N	N	N

F2	Gender	CKD (age)	Kidney failure (age)	Hyperuricemia	Gout (age)
p.C170Y I.1	M	Y	Y (69y)	Y	Y
p.C170Y II.1	F	Y	N (73y: eGFR 33mL/min; 86y: no ESKD)	Y	N
p.C170Y II.2	F	Y	Y (84y)	Y	N
p.C170Y III.1	F	Y (33y)	N (54y)	Y	N

M, male; F, female; Y, yes; N, no; NA, not available; CKD, chronic kidney disease; eGFR, estimated glomerular filtration rate.
* Nephrectomy for clear cell carcinoma – abundant hematuria

Appendix Table S3: In silico analysis of selected *UMOD* missense variants.

Genomic coordinates (GRCh38)	Nucleotide change	Predicted amino acid change	Control & patient databases*	Pathogenicity predictions¥	Comment	ACMG classification (PMID 25741868)
16:20348792:C:T	c.509G>A	p.(Cys170Tyr)	0¶	Pathogenic computational verdict (7 path. vs. 4 ben. predictions), REVEL metascore: 0.63†	Not in ClinVar; located between EGF-like 3 domain and D8C UniProt classifies this variant as Pathogenic, associated with Tubulointerstitial kidney disease, autosomal dominant, 1.	**Likely Pathogenic (PM2, PP2, PP3, PP5, PP1)**
16:20348748:G:T	c.553C>A	p.(Arg185Ser)	0	Pathogenic computational verdict (9 path. vs. 2 ben. predictions), REVEL metascore: 0.84†	Not in ClinVar; located between EGF-like 3 domain and D8C; inside a mutational hot-spot# UniProt classifies this variant as Pathogenic, associated with Tubulointerstitial kidney disease, autosomal dominant, 1.	**Pathogenic (PM1, PM5, PM2, PP2, PP3, PP5, PP1)**

UMOD transcript: NM_001008389.3

* Includes the Genome Aggregation Database (gnomAD) (Karczewski *et al*, 2020), the UK Biobank (Van Hout *et al*, 2020), the Genomics England 100,000 Genomes Project (Turro *et al*, 2020) and the UK Rare Disease Registry (RaDaR) (https://ukkidney.org/rare-renal/radar).

¶ Has been reported before in 1 additional French family with slowly progressive CKD (2 individuals with 72y & 73y not yet in ESKD) (Dahan *et al*, 2003)

¥ Generated using Varsome (Kopanos et al, 2019).

† REVEL, rare exome variant ensemble learner (7) (a score > 0.75 corresponds to a sensitivity of ~0.5 and a specificity of ~0.95 for pathogenic variants in the training dataset).

#Hot-spot of length 17 amino-acids has 9 missense/in-frame/non-synonymous variants (5 pathogenic, 3 uncertain, and 1 benign), which qualifies as a dense hot-spot (Ioannidis et al, 2016).

Abbreviations: path., pathogenic; ben., benign; EGF-like, epidermal growth factor-like domain; D8C, cysteine-rich domain of unknown function.

Appendix Table S4: Clinical and biochemical parameters of *Umod*^{C171Y} mice.

	1 month			4 months		
Parameter	*Umod*$^{+/+}$ n=9	*Umod*$^{C17Y/+}$ n=16	*Umod*$^{C171Y/C171Y}$ n=5	*Umod*$^{+/+}$ n=5	*Umod*$^{C17Y/+}$ n=11	*Umod*$^{C171Y/C171Y}$ n=7
Body weight (BW), g	19.7 ± 0.7	20.2 ± 0.6	19.1 ± 1.5	25.6 ± 1.5	28.3 ± 1.0	27.4 ± 1.5
Water intake, µL·min^{-1}·g BW^{-1}	0.23 ± 0.03	0.27 ± 0.01	0.29 ± 0.02	0.17 ± 0.02	0.14 ± 0.01	0.09 ± 0.02*
Urine						
Diuresis, µL·min^{-1}·g BW^{-1}	0.07 ± 0.02	0.05 ± 0.01	0.04 ± 0.01	0.05 ± 0.01	0.05 ± 0.01	0.05 ± 0.01
Na^+, g·g creat^{-1}	5.6 ± 0.3	5.7 ± 0.2	7.2 ± 0.7	4.5 ± 0.6	6.6 ± 0.4*	4.9 ± 0.7
K^+, g·g creat^{-1}	19.5 ± 1.0	20.1 ± 0.6	23.6 ± 2.0	15.7 ± 0.9	19.2 ± 1.0	15.7 ± 1.0
Cl^-, g·g creat^{-1}	14.4 ± 0.8	14.3 ± 0.4	17.9 ± 1.0*	9.8 ± 0.8	12.6 ± 1.0	10.1 ± 0.8
Ca^{2+}, g·g creat^{-1}	0.14 ± 0.02	0.14 ± 0.01	0.17 ± 0.02	0.17 ± 0.04	0.09 ± 0.01*	0.17 ± 0.02
Mg^{2+}, g·g creat^{-1}	1.32 ± 0.06	1.24 ± 0.08	1.39 ± 0.04	0.95 ± 0.04	1.03 ± 0.03	1.02 ± 0.07
Creatinine, mg·dL^{-1}	44 ± 3	43 ± 2	32 ± 3*	41 ± 5	32 ± 2	35 ± 5
FE_{UA},%	1.16 ± 0.26	0.97 ± 0.12	1.41 ± 0.34	0.59 ± 0.11	-	-
Osmolality, mOsm·kg H_2O^{-1}	1854 ± 85	1816 ± 93	1648 ± 132	1476 ± 184	1364 ± 109	1284 ± 188
Plasma	n=9	n=21	n=9	n=16	n=20	n=24
Na^+, mmol·L^{-1}	147 ± 2	146 ± 1	148 ± 1	147 ± 1	149 ± 1	149 ± 1
Cl^-, mmol·L^{-1}	108 ± 1	108 ± 2	108 ± 2	111 ± 1	110 ± 0.8	111 ± 1
Ca^{2+}, mmol·L^{-1}	2.8 ± 0.04	2.8 ± 0.05	2.8 ± 0.6	2.5 ± 0.05	2.5 ± 0.03	2.50 ± 0.3
Creatinine, mg·dL^{-1}	0.14 ± 0.02	0.13 ± 0.01	0.15 ± 0.03	0.12 ± 0.01	0.13 ± 0.01	0.15 ± 0.01
BUN, mg·dL^{-1}	21 ± 2	19 ± 1	21 ± 1	20 ± 2	25 ± 1*	29 ± 1***
Uric acid, mg·dL^{-1}	6.4 ± 0.4	5.9 ± 0.3	5.2 ± 0.4	5.2 ± 0.5	4.6 ± 0.4	4.0 ± 0.3
Osmolality, mOsm·kg H_2O^{-1}	351 ± 3	343 ± 3	347 ± 4	335 ± 3	342 ± 2*	343 ± 2

Values are presented as average ± SEM. *$P < 0.05$, ***$P < 0.001$, versus age matched *Umod*$^{+/+}$ mice. n: number of animals, FEUA: fractional excretion of uric acid, BUN: blood urea nitrogen.

Appendix Table S5: Clinical and biochemical parameters of *Umod*^{R186S} mice.

	1 month			4 months		
Parameter	*Umod*$^{+/+}$ n=15	*Umod*$^{R186S/+}$ n=18	*Umod*$^{R186S/R186S}$ n=12	*Umod*$^{+/+}$ n=10	*Umod*$^{R186S/+}$ n=13	*Umod*$^{R186S/R186S}$ n=7
Body weight (BW), g	16.5 ± 0.6	16.4 ± 0.6	16.4 ± 0.6	26.3 ± 1.4	23.3 ± 1.0	26.5 ± 0.9
Water intake, µL·min^{-1}·g BW^{-1}	0.29 ± 0.02	0.27 ± 0.02	0.28 ± 0.03	0.15 ± 0.01	0.31 ± 0.02***	0.44 ± 0.04***
Urine						
Diuresis, µL·min^{-1}·g BW^{-1}	0.041 ± 0.006	0.059 ± 0.009	0.14 ± 0.04*	0.046 ± 0.007	0.12 ± 0.01***	0.23 ± 0.02***
Na^+, g·g creat^{-1}	5.8 ± 0.6	6.3 ± 0.7	6.4 ± 0.8	5.6 ± 0.3	5.7 ± 0.5	4.7 ± 0.6
K^+, g·g creat^{-1}	27.7 ± 1.3	23.8 ± 0.9*	27.06 ± 1.1	19.7 ± 1.2	21.4 ± 1.16	19.4 ± 0.6
Cl^-, g·g creat^{-1}	19.8 ± 1.2	17.5 ± 1.0	21.3 ± 1.1	14.5 ± 1.1	15.9 ± 1.0	14.2 ± 0.7
Ca^{2+}, g·g creat^{-1}	0.15 ± 0.02	0.28 ± 0.04*	0.24 ± 0.03*	0.08 ± 0.07	0.21 ± 0.02#	0.20 ± 0.03***
Mg^{2+}, g·g creat^{-1}	2.2 ± 0.9	2.0 ± 0.1	2.3 ± 0.1	1.3 ± 0.1	1.41 ± 0.13	1.65 ± 0.08
Creatinine, mg·dL^{-1}	43 ± 3	34 ± 3	29 ± 3**	50 ± 2	25 ± 2#	15 ± 1#
FE_{UA},%	1.16 ± 0.26	1.18 ± 0.31	0.72 ± 0.36	0.25 ± 0.1	0.74 ± 0.4***	0.16 ± 0.05**
Osmolality, mOsm·kg H_2O^{-1}	2227 ± 186	1647 ± 168*	1440 ± 152**	2012 ± 132	958 ± 58#	583 ± 20#
Plasma	n=9	n=6	n=13	n=23	n=24	n=14
Na^+, mmol·L^{-1}	149 ± 2	149 ± 1	149 ± 1	147 ± 1	149 ± 1*	153 ± 1***
Cl^-, mmol·L^{-1}	109 ± 1	109 ± 1	108 ± 1	119 ± 1	108 ± 1	107 ± 1*
Ca^{2+}, mmol·L^{-1}	2.72 ± 0.05	2.63 ± 0.06	2.64 ± 0.06	2.50 ± 0.03	2.51 ± 0.03	2.65 ± 0.04*
Creatinine, mg·dL^{-1}	0.17 ± 0.04	0.12 ± 0,01	0.15 ± 0.01	0.11 ± 0.01	0.14 ± 0.01*	0.18 ± 0.01***
BUN, mg·dL^{-1}	19 ± 1	33 ± 4***	43 ± 4#	21 ± 1	55 ± 2#	70 ± 2#
Uric acid, mg·dL^{-1}	6.6 ± 0.7	5.2 ± 1.1	5.9 ± 0.5	5.4 ± 0.3	4.8 ± 0.4	5.1 ± 0.8
Osmolality, mOsm·kg H_2O^{-1}	353 ± 4	351 ± 4	356 ± 3	340 ± 2	355 ± 2#	366 ± 3#

Values are presented as average ± SEM. *$P < 0.05$, **$P < 0.01$, ***$P < 0.001$, #$P < 0.0001$ versus age matched *Umod*$^{+/+}$ mice.
n: number of animals, FE_{UA}: fractional excretion of uric acid, BUN: blood urea nitrogen.

Appendix Table S6: Clinical and biochemical parameters of *Umod*$^{R186S/-}$ mice.

	1 month			4 months		
Parameter	*Umod*$^{+/+}$ n=11	*Umod*$^{R186S/+}$ n=10	*Umod*$^{R186S/-}$ n=9	*Umod*$^{+/+}$ n=8	*Umod*$^{R186S/+}$ n=7	*Umod*$^{R186S/-}$ n=13
Body weight (BW), g	16.1 ± 0.7	15.6 ± 0.6	16.6 ± 0.6	29.2 ± 1.7	26.6 ± 1.3	29.4 ± 0.6
Water intake, µL·min^{-1}·g BW^{-1}	0.36 ± 0.03	0.30 ± 0.01	0.33 ± 0.02	0.15 ± 0.02	0.29 ± 0.02***	0.25 ± 0.02**
Urine						
Diuresis, µL·min^{-1}·g BW^{-1}	0.048 ± 0.008	0.057 ± 0.009	0.04 ± 0.01	0.03 ± 0.01	0.13 ± 0.02***	0.11 ± 0.01#
Na^+, g·g creat^{-1}	8.3 ± 0.5	9.0 ± 0.4	9.0 ± 0.6	3.2 ± 0.5	4.0 ± 0.3	3.9 ± 0.3
K^+, g·g creat^{-1}	27.8 ± 0.9	30.0 ± 0.8	30.8 ± 1.4	18.7 ± 1.2	19.1 ± 1.2	18.5 ± 0.8
Cl^-, g·g creat^{-1}	23.9 ± 0.8	25.5 ± 1.0	26.3 ± 1.4	10.8 ± 0.4	12.4 ± 1.0	11.6 ± 0.8
Ca^{2+}, g·g creat^{-1}	0.23 ± 0.03	0.27 ± 0.02	0.28 ± 0.03	0.14 ± 0.02	0.22 ± 0.01**	0.22 ± 0.01**
Mg^{2+}, g·g creat^{-1}	2.0 ± 0.2	2.2 ± 0.1	2.2 ± 0.2	1.2 ± 0.1	1.43 ± 0.07	1.32 ± 0.09
Creatinine, mg·dL^{-1}	35.2 ± 3.0	30.7 ± 1.4	37.2 ± 4.1	44.2 ± 5.5	21.7 ± 2.3**	20.3 ± 1.1#
FE_{UA},%	-	-	-	0.55 ± 0.09	0.14 ± 0.02**	0.16 ± 0.03**
Osmolality, mOsm·kg H_2O^{-1}	1855 ± 120	1766 ± 81	2091 ± 217	1577 ± 201	771 ± 42**	731 ± 29#
Plasma	n=13	n=10	n=11	n=14	n=15	n=20
Na^+, mmol·L^{-1}	145.9 ± 0.8	145.3 ± 0.8	145.1 ± 0.7	147.3 ± 0.7	149.1 ± 0.5*	148.2 ± 0.5
Cl^-, mmol·L^{-1}	107.8 ± 0,7	107.1 ± 0.5	110.3 ± 0.9	110.0 ± 1.1	107.1 ± 0.7*	106 .6 ± 0.3**
Ca^{2+}, mmol·L^{-1}	2.67 ± 0.07	2.82 ± 0.05	2.77 ± 0.05	2.46 ± 0.05	2.62 ± 0.03**	2.62 ± 0.03**
Creatinine, mg·dL^{-1}	0.15 ± 0.02	0.142 ± 0.02	0.17 ± 0.03	0.10 ± 0.02	0.17 ± 0.02*	0.16 ± 0.01*
BUN, mg·dL^{-1}	19 ± 1	32 ± 2#	32 ± 1.#	20 ± 1.0	53 ± 4 #	56 ± 1.#
Uric acid, mg·dL^{-1}	3.3 ± 0.5	4.0 ± 0.9	4.8 ± 0.5	4.1 ± 0.3	4.1 ± 0.4	3.8 ± 0.4
Osmolality, mOsm·kg H_2O^{-1}	341 ± 4	353 ± 3	355 ± 4*	338 ± 3	353 ± 3**	357 ± 3#

Values are presented as average ± SEM. *$P < 0.05$, **$P < 0.01$, ***$P < 0.001$, #$P < 0.0001$ versus age-matched *Umod*$^{+/+}$ mice or ŧ $P \leq 0.05$ versus age-matched *Umod*$^{R186S/+}$ mice. n: number of animals, FE_{UA}: fractional excretion of uric acid, BUN: blood urea nitrogen.

Appendix Table S7: Clinical and biological parameters of 4-month *Umod* KI mice per gender.

	Female			Male		
Plasma	*Umod*$^{+/+}$ n=10	*Umod*$^{C171Y/+}$ n=12	*Umod*$^{C171Y/C171Y}$ n=17	*Umod*$^{+/+}$ n=5	*Umod*$^{C171Y/+}$ n=8	*Umod*$^{C171Y/C171Y}$ n=7
BUN, mg·dL^{-1}	18 ± 2	23 ± 1	27 ± 2**	19 ± 2	28 ± 2*	36 ± 2***

Urine	*Umod*$^{+/+}$ n=5	*Umod*$^{R186S/+}$ n=9	*Umod*$^{R186S/R186S}$ n=3	*Umod*$^{+/+}$ n=5	*Umod*$^{R186S/+}$ n=4	*Umod*$^{R186S/R186S}$ n=4
Diuresis, µL·min^{-1}·g BW^{-1}	0.05 ± 0.01	0.11 ± 0.02[a]	0.3 ± 0.00[a]	0.04 ± 0.01	0.14 ± 0.01**	0.21 ± 0.02#
Osmolality, mOsm·kg H_2O^{-1}	2087 ± 246	950 ± 87***	564 ± 50***	1936 ± 157	974 ± 47***	598 ± 17#
Plasma	n=17	n=14	n=7	n=7	n=11	n=7
Creatinine, mg·dL^{-1}	0.10 ± 0.01[b]	0.18 ± 0.01[c]#	0.21 ± 0.02#	0.14 ± 0.02	0.10 ± 0.02[c]	0.156 ± 0.004
BUN, mg·dL^{-1}	19 ± 1	53 ± 3#	71 ± 3#	25 ± 1	58 ± 3#	70 ± 3#

Urine	*Umod*$^{+/+}$ n=5	*Umod*$^{R186S/+}$ n=9	*Umod*$^{R186S/R186S}$ n=3	*Umod*$^{+/+}$ n=5	*Umod*$^{R186S/+}$ n=4	*Umod*$^{R186S/R186S}$ n=4
Diuresis, µL·min^{-1}·g BW^{-1}	0.008 ± 0.001	0.13 ± 0.06	0.14 ± 0.03	0.04 ± 0.02	0.13 ± 0.02**	0.10 ± 0.01**
Osmolality, mOsm·kg H_2O^{-1}	2046 ± 438	752 ± 64	701 ± 89	1296 ± 140	778 ± 62***	736 ± 31#
Plasma	n=6	n=6	n=10	n=8	n=9	n=10
Creatinine, mg·dL^{-1}	0.10 ± 0.03[d]	0.17 ± 0.02	0.17 ± 0.02	0.10 ± 0.03[d]	0.17 ± 0.03[d]	0.15 ± 0.02
BUN, mg·dL^{-1}	18 ± 1	54 ± 4#	56 ± 4#	22 ± 1	52 ± 6#	56 ± 2#

Values are presented as average ± SEM. One-way ANOVA with Tukey's post hoc per gender. *P<0.05, **P<0.01, ***P<0.001, #P<0.0001 versus gender-matched *Umod*$^{+/+}$ mice, n: number of animals, BUN: blood urea nitrogen. [a]2 samples were not available for analysis, [b]3 samples were undetectable. [c]1 sample was undetectable, [d]2 samples were undetectable.

Appendix Table S8: Top 50 DEGs in *Umod*$^{R186S/+}$ kidneys at 1 month.

Symbol	Gene name	Fold change (log2)	FDR (-log10)
Lcn2	Lipocalin 2	4.09	100.44
Atf5	Activating transcription factor 5	2.61	52.02
Trib3	Tribbles pseudokinase 3	4.04	37.43
Asns	Asparagine synthetase	2.39	33.55
Mthfd2	Methylenetetrahydrofolate dehydrogenase (NAD+ dependent), methenyltetrahydrofolate cyclohydrolase	2.31	27.30
Akr1b8	Aldo-keto reductase family 1, member B8	2.21	20.17
Cxcl10	Chemokine (C-X-C motif) ligand 10	2.92	19.70
Stc2	Stanniocalcin 2	2.29	19.52
Aldh18a1	Aldehyde dehydrogenase 18 family, member A1	2.08	18.88
Angptl6	Angiopoietin-like 6	2.33	14.69
Aldh1l2	Aldehyde dehydrogenase 1 family, member L2	1.87	14.36
Slc7a11	Solute carrier family 7 (cationic amino acid transporter, y+ system), member 11	2.56	13.53
Mt2	Metallothionein 2	1.76	13.17
Slc7a3	Solute carrier family 7 (cationic amino acid transporter, y+ system), member 3	2.62	12.81
Nupr1	Nuclear protein transcription regulator 1	1.45	12.61
Cbr3	Carbonyl reductase 3	2.15	12.12
Arhgap36	Rho GTPase activating protein 36	2.76	11.99
Soat2	Sterol O-acyltransferase 2	2.56	11.48
Pappa	Pregnancy-associated plasma protein A	1.91	11.33
Slc38a1	Solute carrier family 38, member 1	1.40	11.25
Wnt10a	Wingless-type MMTV integration site family, member 10A	2.65	10.75
Gabrp	Gamma-aminobutyric acid (GABA) A receptor, pi	2.51	10.74
Loxl4	Lysyl oxidase-like 4	1.66	9.76
Lgals3	Lectin, galactose binding, soluble 3	1.24	9.48
Fam129a	Family with sequence similarity 129, member A	1.32	8.13
Egf	Epidermal growth factor	-2.00	40.86
Umod	Uromodulin	-1.74	24.75
Car3	Carbonic anhydrase 3	-2.01	14.36
Gm36797	Predicted gene, 36797	-2.65	13.46
Gm32960	Predicted gene, 32960	-1.74	13.17
Kcnt1	Potassium channel, subfamily T, member 1	-1.87	9.55
Wfdc15b	WAP four-disulfide core domain 15B	-1.23	7.59
Azgp1	Aalpha-2-glycoprotein 1, zinc	-1.47	6.76
Dusp15	Dual specificity phosphatase-like 15	-1.46	6.47
Cyp2a4	Cytochrome P450, family 2, subfamily a, polypeptide 4	-1.04	6.32
Slc6a6	Solute carrier family 6 (neurotransmitter transporter, taurine), member 6	-0.63	5.88
Atp8b4	ATPase, class I, type 8B, member 4	-1.56	5.67
Fam107a	Family with sequence similarity 107, member A	-0.99	5.53
Slco1a6	Solute carrier organic anion transporter family, member 1a6	-0.74	4.95
Tmem207	Transmembrane protein 207	-1.39	4.87
BC040756	cDNA sequence BC040756	-0.87	4.74
Pex5l	Peroxisomal biogenesis factor 5-like	-1.48	4.49
Esrrb	Estrogen related receptor, beta	-0.97	4.49
Cwh43	Cell wall biogenesis 43 C-terminal homolog	-0.78	4.49
6330410L21Rik	RIKEN cDNA 6330410L21 gene	-1.35	4.41
Ugt8a	UDP galactosyltransferase 8A	-0.85	4.41
Omd	Osteomodulin	-1.12	4.19
Rnf169	Ring finger protein 169	-0.88	4.18
Dok2	Docking protein 2	-1.13	4.13
Perm1	PPARGC1 and ESRR induced regulator, muscle 1	-1.36	4.09

FDR: False discovery rate-adjusted *P* value (Benjamini-Hochberg correction).

Appendix Table S9: Top 50 DEGs in *Umod*$^{R186S/+}$ kidneys at 4 months.

Symbol	Gene name	Fold change (log2)	FDR (-log10)
Lcn2	Lipocalin 2	4.23	114.29
Arhgap36	Rho GTPase activating protein 36	6.04	66.64
Slc7a11	Solute carrier family 7 (cationic amino acid transporter, y+ system), member 11	4.91	53.68
Akr1b8	Aldo-keto reductase family 1, member B8	3.36	52.89
Nefl	Neurofilament, light polypeptide	3.98	52.36
Dpt	Dermatopontin	3.03	49.97
Cbr3	Carbonyl reductase 3	4.02	47.22
Atf5	Activating transcription factor 5	2.38	44.14
Ppp2r2c	Protein phosphatase 2, regulatory subunit B, gamma	4.49	37.30
Trib3	Tribbles pseudokinase 3	3.78	34.16
B4galnt2	Beta-1,4-N-acetyl-galactosaminyl transferase 2	3.78	32.79
Aldh18a1	Aldehyde dehydrogenase 18 family, member A1	2.62	30.76
Asns	Asparagine synthetase	2.14	28.48
Stc2	Stanniocalcin 2	2.84	26.86
Gabrp	Gamma-aminobutyric acid (GABA) A receptor, pi	3.51	23.20
Aldh1l2	Aldehyde dehydrogenase 1 family, member L2	2.25	22.19
Abcc3	ATP-binding cassette, sub-family C (CFTR/MRP), member 3	2.21	21.80
Smoc2	SPARC related modular calcium binding 2	2.04	21.77
Astn2	Astrotactin 2	2.22	21.40
Fcrls	Fc receptor-like S, scavenger receptor	3.50	20.52
Kif1a	Kinesin family member 1A	2.90	20.50
Lyz2	Lysozyme 2	1.98	20.30
Gm32857	Predicted gene, 32857	3.62	20.28
Mrc1	Mannose receptor, C type 1	1.89	20.28
Mthfd2	Methylenetetrahydrofolate dehydrogenase (NAD+ dependent), methenyltetrahydrofolate cyclohydrolase	1.92	19.46
Egf	Epidermal growth factor	-3.30	115.22
Gpx6	Glutathione peroxidase 6	-2.57	58.29
Kcnt1	Potassium channel, subfamily T, member 1	-4.04	45.73
Umod	Uromodulin	-2.13	38.09
Wfdc15b	WAP four-disulfide core domain 15B	-2.21	28.02
Tmem207	Transmembrane protein 207	-2.62	20.68
Aldoc	Aldolase C, fructose-bisphosphate	-1.67	17.42
Dusp15	Dual specificity phosphatase-like 15	-2.27	15.75
Gm36797	Predicted gene, 36797	-2.76	14.99
Gm32960	Predicted gene, 32960	-1.76	14.00
Ppp1r1a	Protein phosphatase 1, regulatory inhibitor subunit 1A	-1.13	13.72
Pex5l	Peroxisomal biogenesis factor 5-like	-2.36	12.85
Perm1	PPARGC1 and ESRR induced regulator, muscle 1	-2.21	12.77
Lrrc66	Leucine rich repeat containing 66	-1.65	12.49
Ckb	Creatine kinase, brain	-1.36	11.45
Ank2	Ankyrin 2, brain	-1.18	10.87
Mfsd4a	Major facilitator superfamily domain containing 4A	-1.10	10.75
6330410L21Rik	RIKEN cDNA 6330410L21 gene	-2.09	10.48
Pcsk6	Proprotein convertase subtilisin/kexin type 6	-1.27	10.45
Slc6a12	Solute carrier family 6 (neurotransmitter transporter, betaine/GABA), member 12	-1.90	9.48
Spag5	Sperm associated antigen 5	-1.78	9.48
Clcnka	Chloride channel, voltage-sensitive Ka	-1.29	9.46
Gcgr	Glucagon receptor	-1.19	9.23
Pla1a	Phospholipase A1 member A	-1.00	8.76
Aqp4	Aquaporin 4	-1.37	8.33

FDR: False discovery rate-adjusted *P* value (Benjamini-Hochberg correction).

Appendix Table S10: Top 50 DEGs in *Umod*$^{C171Y/+}$ kidneys at 4 months.

Symbol	Gene name	Fold change (log2)	FDR (-log10)
Jun	Jun proto-oncogene	2.86	23.00
Btg2	BTG anti-proliferation factor 2	2.72	22.27
Ccn1	Cellular communication network factor 1	3.29	18.39
Fos	FBJ osteosarcoma oncogene	3.38	16.46
Ier2	Immediate early response 2	2.68	15.92
Zfp36	Zinc finger protein 36	1.96	13.97
Nr4a2	Nuclear receptor subfamily 4, group A, member 2	2.94	13.51
Ier3	Immediate early response 3	2.15	13.47
Nr4a1	Nuclear receptor subfamily 4, group A, member 1	2.79	10.13
Fosb	FBJ osteosarcoma oncogene B	2.03	6.90
Snord14e	Small nucleolar RNA, C/D box 14°	1.77	6.43
Csrnp1	Cysteine-serine-rich nuclear protein 1	1.65	6.32
Gdf15	Growth differentiation factor 15	1.87	6.32
Ccn2	Cellular communication network factor 2	1.18	6.18
Gm30591	Predicted gene, 30591	2.09	5.88
Tob1	Transducer of ErbB-2.1	1.14	5.47
Egr1	Early growth response 1	1.94	4.77
Gm17971	Predicted gene, 17971	1.28	4.69
Snord14d	Small nucleolar RNA, C/D box 14D	1.77	4.11
Egr3	Early growth response 3	1.76	3.99
Rasd1	RAS, dexamethasone-induced 1	1.29	3.68
Dusp6	Dual specificity phosphatase 6	1.17	3.67
Ighv5-9	Immunoglobulin heavy variable 5-9	1.47	3.31
Ch25h	Cholesterol 25-hydroxylase	1.68	3.27
Ighg2b	Immunoglobulin heavy constant gamma 2B	1.70	2.93
mt-Tl1	tRNA leucine 1, mitochondrial	-1.21	4.57
Gm30238	predicted gene, 30238	-1.60	3.27
Igkv13-85	immunoglobulin kappa chain variable 13-85	-1.12	2.21
Cyp2d26	cytochrome P450, family 2, subfamily d, polypeptide 26	-1.32	2.16
Lpl	lipoprotein lipase	-1.38	2.14
Synpr	synaptoporin	-1.30	2.06
Mir6236	microRNA 6236	-1.51	2.05
1700067K01Rik	RIKEN cDNA 1700067K01 gene	-1.01	1.91
Atp1a2	ATPase, Na+/K+ transporting, alpha 2 polypeptide	-1.20	1.82
Itih1	inter-alpha trypsin inhibitor, heavy chain 1	-1.09	1.76
Apoc1	apolipoprotein C-I	-1.04	1.55
Adig	adipogenin	-0.91	5.38
Slc5a1	solute carrier family 5 (sodium/glucose cotransporter), member 1	-0.64	3.17
Rn18s-rs5	18s RNA, related sequence 5	-0.94	2.83
LOC108167485	putative uncharacterized protein FLJ37770 pseudogene	-0.87	2.11
Gm17597	predicted gene, 17597	-0.83	2.11
Mri1	methylthioribose-1-phosphate isomerase 1	-0.51	1.92
Gm34472	predicted gene, 34472	-0.91	1.73
Gm28023	predicted gene, 28023	-0.65	1.56
Tcf24	transcription factor 24	-0.58	1.37
Ugt3a1	UDP glycosyltransferases 3 family, polypeptide A1	-0.39	1.29
Cfd	complement factor D (adipsin)	-1.26	1.25
AI429214	expressed sequence AI429214	-0.75	1.25
AA536875	expressed sequence AA536875	-0.92	1.15
Gm15564	predicted gene 15564	-1.22	1.15

FDR: False discovery rate-adjusted *P* value (Benjamini-Hochberg correction).

Appendix Table S11: Top 50 DEGs in *Umod*$^{R186S/+}$ compared to *Umod*$^{C171Y/+}$ kidneys at 1 month.

Symbol	Gene name	Fold change (log2)	FDR (-log10)
Lcn2	Lipocalin 2	4.16	99.72
Atf5	Activating transcription factor 5	2.67	53.11
Asns	Asparagine synthetase	2.36	32.01
Trib3	Tribbles pseudokinase 3	3.65	30.80
Mthfd2	Methylenetetrahydrofolate dehydrogenase (NAD+ dependent), methenyltetrahydrofolate cyclohydrolase	2.28	26.20
Stc2	Stanniocalcin 2	2.45	21.46
Akr1b8	Aldo-keto reductase family 1, member B8	2.29	21.33
Cxcl10	Chemokine (C-X-C motif) ligand 10	2.94	19.82
Aldh18a1	Aldehyde dehydrogenase 18 family, member A1	2.16	19.82
Cbr3	Carbonyl reductase 3	2.45	14.95
Arhgap36	Rho GTPase activating protein 36	2.99	13.98
Nupr1	Nuclear protein transcription regulator 1	1.44	12.23
Angptl6	Angiopoietin-like 6	2.13	12.16
Samd5	Sterile alpha motif domain containing 5	2.49	11.82
Soat2	Sterol O-acyltransferase 2	2.62	11.70
Aldh1l2	Aldehyde dehydrogenase 1 family, member L2	1.71	11.70
Gabrp	Gamma-aminobutyric acid (GABA) A receptor, pi	2.62	11.40
Slc7a11	Solute carrier family 7 (cationic amino acid transporter, y+ system), member 11	2.36	11.40
Lgals3	Lectin, galactose binding, soluble 3	1.34	11.16
Slc7a3	Solute carrier family 7 (cationic amino acid transporter, y+ system), member 3	2.44	10.98
Wnt10a	Wingless-type MMTV integration site family, member 10A	2.58	10.07
Mt2	Metallothionein 2	1.55	10.03
Pappa	Pregnancy-associated plasma protein A	1.81	9.98
Slc38a1	Solute carrier family 38, member 1	1.31	9.58
Serpina10	Serine (or cysteine) peptidase inhibitor, clade A (alpha-1 antiproteinase, antitrypsin), member 10	2.02	9.52
Egf	Epidermal growth factor	-1.89	36.25
Umod	Uromodulin	-1.63	21.44
Azgp1	Alpha-2-glycoprotein 1, zinc	-1.83	11.19
Car3	Carbonic anhydrase 3	-1.80	11.16
Kcnt1	Potassium channel, subfamily T, member 1	-1.93	10.25
Gm36797	Predicted gene, 36797	-2.32	9.74
Gm34472	Predicted gene, 34472	-1.21	8.77
Gm34861	Predicted gene, 34861	-1.54	8.63
Cyp2a4	Cytochrome P450, family 2, subfamily a, polypeptide 4	-1.14	7.88
Tc2n	Tandem C2 domains, nuclear	-1.37	7.77
Agps	Alkylglycerone phosphate synthase	-1.01	7.08
Ksr2	Kinase suppressor of ras 2	-1.10	7.05
Wfdc15b	WAP four-disulfide core domain 15B	-1.18	7.01
Gm32960	Predicted gene, 32960	-1.30	6.72
Trpm6	Transient receptor potential cation channel, subfamily M, member 6	-1.26	6.64
Atp8b4	ATPase, class I, type 8B, member 4	-1.58	5.95
Syn3	Synapsin III	-1.33	5.87
Col19a1	Collagen, type XIX, alpha 1	-1.60	5.79
Idi1	Isopentenyl-diphosphate delta isomerase	-1.21	5.77
Slco1a1	Solute carrier organic anion transporter family, member 1a1	-1.63	5.67
Ubiad1	UbiA prenyltransferase domain containing 1	-1.26	5.31
Dusp15	Dual specificity phosphatase-like 15	-1.33	5.23
Gm38481	Predicted gene, 38481	-1.22	4.87
Gm7537	Predicted gene 7537	-1.27	4.81
Perm1	PPARGC1 and ESRR induced regulator, muscle 1	-1.43	4.80

FDR: False discovery rate-adjusted *P* value (Benjamini-Hochberg correction).

Appendix Table S12: Top 50 DEGs in *Umod*$^{R186S/+}$ compared to *Umod*$^{C171Y/+}$ at 4 months.

Symbol	Gene name	Fold change (log2)	FDR (-log10)
Lcn2	Lipocalin 2	4.73	132.87
Akr1b8	Aldo-keto reductase family 1, member B8	3.95	70.59
Arhgap36	Rho GTPase activating protein 36	5.99	65.97
Slc7a11	Solute carrier family 7 (cationic amino acid transporter, y+ system), member 11	4.76	51.56
Dpt	Dermatopontin	2.99	49.40
Nefl	Neurofilament, light polypeptide	3.41	42.31
Trib3	Tribbles pseudokinase 3	4.00	37.82
Cbr3	Carbonyl reductase 3	3.34	35.67
Atf5	Activating transcription factor 5	2.10	35.22
Ppp2r2c	Protein phosphatase 2, regulatory subunit B, gamma	4.32	35.17
B4galnt2	Beta-1,4-N-acetyl-galactosaminyl transferase 2	3.62	30.75
Asns	Asparagine synthetase	2.21	30.44
Gabrp	Gamma-aminobutyric acid (GABA) A receptor, pi	4.00	29.49
Aldh18a1	Aldehyde dehydrogenase 18 family, member A1	2.32	25.09
Gsta4	Glutathione S-transferase, alpha 4	1.57	22.20
Stc2	Stanniocalcin 2	2.40	20.49
Kif1a	Kinesin family member 1A	2.88	20.41
Gm32857	Predicted gene, 32857	3.64	20.41
Col18a1	Collagen, type XVIII, alpha 1	1.05	20.29
Abcc3	ATP-binding cassette, sub-family C (CFTR/MRP), member 3	2.05	19.39
Astn2	Astrotactin 2	2.08	19.23
Slc38a1	Solute carrier family 38, member 1	1.78	19.08
Mthfd2	Methylenetetrahydrofolate dehydrogenase (NAD+ dependent), methenyltetrahydrofolate cyclohydrolase	1.89	19.08
Eda2r	Ectodysplasin A2 receptor	2.53	18.69
Ugt2b35	UDP glucuronosyltransferase 2 family, polypeptide B35	3.39	18.43
Egf	Epidermal growth factor	-3.06	99.15
Gpx6	Glutathione peroxidase 6	-2.50	55.12
Kcnt1	Potassium channel, subfamily T, member 1	-3.94	43.24
Umod	Uromodulin	-2.09	36.46
Jun	Jun proto-oncogene	-3.19	30.59
Zfp36	Zinc finger protein 36	-2.62	27.09
Btg2	BTG anti-proliferation factor 2	-2.90	26.64
Tmem207	Transmembrane protein 207	-2.71	22.26
Ckb	Creatine kinase, brain	-1.84	22.20
Ier2	Immediate early response 2	-2.95	20.44
Wfdc15b	WAP four-disulfide core domain 15B	-1.90	20.41
Nr4a1	Nuclear receptor subfamily 4, group A, member 1	-3.63	19.45
Pex5l	Peroxisomal biogenesis factor 5-like	-2.83	19.25
Fos	FBJ osteosarcoma oncogene	-3.41	17.78
Ccn1	Cellular communication network factor 1	-3.15	17.74
Ppp1r1a	Protein phosphatase 1, regulatory inhibitor subunit 1A	-1.27	17.43
Snord14e	Small nucleolar RNA, C/D box 14E	-2.76	17.17
Dusp15	Dual specificity phosphatase-like 15	-2.35	17.14
Csmp1	Cysteine-serine-rich nuclear protein 1	-2.46	17.07
Ier3	Immediate early response 3	-2.28	16.10
Gm36797	Predicted gene, 36797	-2.79	15.52
Nr4a2	Nuclear receptor subfamily 4, group A, member 2	-2.96	14.57
Tob1	Transducer of ErbB-2.1	-1.65	14.36
Ccn2	Cellular communication network factor 2	-1.62	14.05
Gm17971	Predicted gene, 17971	-2.05	14.02

FDR: False discovery rate-adjusted *P* value (Benjamini-Hochberg correction).

Appendix Table S13: List of primary antibodies.

Target Antigen	Host species	Dilution	Cat #	Registry ID	Source
Uromodulin	Sheep	IF 1:300 WB 1:500	K90071C	AB_153128	Meridian Life Science
GRP78	Rabbit	IF 1:300 WB 1:1000	ab21685	AB_2119834	Abcam
β-Actin	Mouse	WB 1:10000	A5441	AB_476744	Sigma-Aldrich
Calnexin	Rabbit	IF 1:300	C4731	AB_476845	Sigma-Aldrich
CD3	Rabbit	IF 1:300	ab16669	AB_443425	Abcam
PERK	Rabbit	WB 1:500	3192	AB_2095847	Cell Signaling Technology
IRE1 (phospho Ser724)	Rabbit	WB 1:500	ab48187	AB_873899	Abcam
IRE1-α	Rabbit	WB 1:500	3294	AB_823545	Cell Signaling Technology
ATF4	Rabbit	WB 1:500	ab105383	AB_10861973	Abcam
eIF2α (phospho Ser51)	Rabbit	WB 1:250	3398	AB_2096481	Cell Signaling Technology
eIF2α	Rabbit	WB 1:500	5324	AB_10692650	Cell Signaling Technology
Lipocalin 2	Rabbit	IF 1:300	ab63929	AB_1140965	Abcam
	Goat	WB 1:500	AF1857	AB_355022	R and D Systems
Cleaved Caspase-3	Rabbit	WB 1:250	9661	AB_2341188	Cell Signaling Technology
Caspase-3	Rabbit	WB 1:1000	9662	AB_331439	Cell Signaling Technology
SQSTM1/p62	Mouse	WB 1:1000	ab56416	AB_945626	Abcam
	Rabbit	IF 1:200	ab109012	AB_2810880	Abcam
S6 Ribosomal Protein (phospho S235/236)	Rabbit	WB 1:500	4858	AB_916156	Cell Signaling Technology
S6 Ribosomal Protein	Rabbit	WB 1:500	2217	AB_331355	Cell Signaling Technology
LC3	Rabbit	IF 1:300 WB 1:500	PM036	AB_2274121	MBL International
GFP	Goat	WB 1:1000	AB0020	AB_2333100	SICGEN
Ubiquitin	Mouse	WB 1:1000	sc-8017	AB_628423	Santa Cruz Biotechnology
F4/80	Rabbit	IF 1:300	70076	AB_2799771	Cell Signaling Technology
LAMP1	Rat	IF 1:300	sc-19992	AB_2134495	Santa Cruz Biotchnology
ATG5	Rabbit	IF 1:300	ab108327	AB_2650499	Abcam

Appendix Table S14: Primers used for real-time RT-PCR analysis.

Gene product	Forward primer (5'-3')	Reverse primer (5'-3')	PCR Product (bp)	Efficiency
18S	GTA ACC CGT TGA ACC CCA TT	CCA TCC AAT CGG TAG TAG CG	151	0.98 ± 0.02
36B4	CTT CAT TGT GGG AGC AGA CA	TTC TCC AGA GCT GGG TTG TT	150	1.02 ± 0.02
Acox1	CTG GTG GGT GGT ATG GTG TC	GTG ACT CAC TTG GGC CTG AA	186	1.03 ± 0.03
Acox2	AAG CCT CAT CCA ACG TGA CC	AAT GCG TTC AGG ACC GTC TT	151	0.99 ± 0.02
Acox3	CAT GTA CGA CTG GTC CCT GG	CCC ATG ACT CAG TTC GGT GA	160	1.02 ± 0.03
Acta2	TGT GCT GGA CTC TGG AGA TG	GAA GGA ATA GCC ACG CTC AG	148	1.03 ± 0.02
Actg1	TGC CCA TCT ATG AGG GCT AC	CCC GTT CAG TCA GGA TCT TC	102	1.03 ± 0.04
Adgre1	CCA GGA GTG GCT TTT GTC TC	GGC TTG GAG AAG TCC TCC TT	152	0.97 ± 0.03
Atf3	CCA GGT CTC TGC CTC AGA AG	CCG ATG GCA GAG GTG TTT AT	151	0.98 ± 0.03
Atf4	CAT GCC AGA TGA GCT CTT GA	GGC AAC CTG GTC GAC TTT TA	145	0.96 ± 0.03
Ccnd1	AGC AGA AGT GCG AAG AGG AG	CAA GGG AAT GGT CTC CTT CA	149	0.98 ± 0.03
Cd68	CCA ACA AAA CCA AGG TCC AG	ATT GTA TTC CAC CGC CAT GT	152	1.03 ± 0.03
Col1a1	GAT CTC CTG GTG CTG ATG GA	GAC CTT GTT TGC CAG GTT CA	156	0.98 ± 0.03
Col3a1	TCC TGG TGG TCC TGG TAC T	TTG CCA GGA GAA CCA CTG TT	154	0.96 ± 0.04
Cpt1a	TGG CAG TCG ACT CAC CTT TC	ACA CCA TAG CCG TCA TCA GC	166	0.98 ± 0.02
Cpt2	TTG ACG CCA TTC AGT TTC AG	GCA GTG CTG CAG GAT TCA TA	148	1.02 ± 0.03
Cryab	ACT TCC CTG AGC CCC TTC TA	CTT GCC GTG GAC CTC AAT CA	186	0.98 ± 0.02
Dnaja4	TGA AGG CAT CGG TGG GAA AA	AGT TCT CAC AGC GGT CCT TG	176	1.02 ± 0.03
Dnajb4	GAC CCT CCC GTC TCA AAC AA	TGA TTT TGG TGC CTT CTT TCC AC	195	1.01 ± 0.02
Ddit3	CCA GGA GGA AGA GGA GGA AG	CCG CTC GTT CTC TTC AGC TA	148	1.02 ± 0.03
Eif2a	ATT ATC ACC ATC CCC GCC AC	GCA GGC ACA GAC AGT CTC AT	166	0.97 ± 0.04
Eif2ak3	GAC TGC GGA GAC AAC AGT GA	GGA CGT TCC TTC CCT AGA CC	173	0.99 ± 0.02
Fn1	GCA AGC CAG TTT CCA TCA AT	CAT TTT TGG GAG TGG TGG TC	150	0.98 ± 0.02
Gapdh	TGC ACC ACC AAC TGC TTA GC	GGA TGC AGG GAT GGG GGA GA	176	1.04 ± 0.03
Hprt1	ACA TTG TGG CCC TCT GTG TG	TTA TGT CCC CCG TTG ACT GA	162	0.99 ± 0.01
Hsp90aa1	CCC GTG AAA TGC TGC AAC AA	GTA CCG CAA CAG CTC TGA AAG	200	0.98 ± 0.03
Hsp90ab1	GAC CTG CCC CTG AAC ATC TC	GGC GTC GGT TAG TGG AAT CT	196	1.04 ± 0.02
Hspa5	CAC TGT GGT ACC CAC CAA GA	GCA GGA GGA ATT CCA GTC AG	149	1.01 ± 0.02
Lcn2	ATG TCA CCT CCA TCC TGG TC	GTG GCC ACT TGC ACA TTG TA	148	0.97 ± 0.03
Lgals3	GCC TAC CCC AGT GCT CCT	TTG CGT TGG GTT TCA CTG TG	151	0.98 ± 0.02
Mki67	TGC AAA GGT AGA GGC TCC AT	CAG GTA GGC CAG AGC AAG T	152	0.98 ± 0.03
Nupr1	ACC CTT CCC AGC AAC CTC TA	TGG AAC TTG GTC AGC AGC TT	187	0.97 ± 0.02
Pcna	TTG GAA TCC CAG AAC AGG AG	ATT GCC AAG CTC TCC ACT TG	155	1.04 ± 0.03
Ppia	CGT CTC CTT CGA GCT GTT TG	CCA CCC TGG CAC ATG AAT C	139	1.02 ± 0.02
Ptprc	GGA GAC CAG GAA GTC TGT GC	GTT CTG GGC TCC TTC CTC TT	145	0.97 ± 0.03
Retreg1	ACT TGA CCA GGC AGA GCT AG	TTT ATC TGT GCT TCG CTG GC	160	1.01 ± 0.02
Rtn3	AGA GTG TGC TTT CCC CTC TC	TCC TCC TCC ACA GAC TGA GA	187	0.99 ± 0.01
Sec61a1	CGT TGG TGG CCT GTG TTA CT	CAC CAT CTG CTG CTC CTT CA	190	1.02 ± 0.03
Sec62	TCT GGC CAG CAG AAA TGA GA	CAG TCA GGT TTG GCA GGA AC	164	0.97 ± 0.02
Slc12a1	ATT GGC CTG AGC GTA GTT GT	AGC AAA GAT CAA GCC TAT TGA CC	150	1.01 ± 0.03
Sqstm1	CCC CAA TGT GAT CTG TGA TG	AAG GGG TTG GGA AAG ATG AG	127	0.99 ± 0.03
Tgfb1	GTG GAA ATC AAC GGG ATC AG	GTT GGT ATC CAG GGC TCT C	150	0.96 ± 0.03
Tlr4	GTG GCC CTA CCA AGT CTC AG	GAC CCA TGA AAT TGG CAC TC	154	1.01 ± 0.02
Umod	TCA GCC TGA AGA CCT CCC TA	GAA AAG CCT CAG TGG ACA GC	156	0.99 ± 0.02
Xbp1s	GCC ATT GTC TGA GAC CAC CT	AGC TGG GGG AAA AGT TCA TT	151	0.98 ± 0.04

Appendix Table S15: RNA-Seq quality and yield.

Sample	Genotype (*Umod*)	Age (months)	Yeld (Mbp)	%Q30	Mean Q
WT_1.1	+/+	1	4'802	91.63	34.75
WT_1.2	+/+	1	6'401	90.87	34.47
WT_1.3	+/+	1	5'373	93.09	35.16
C171Y_1.1	C171Y/+	1	5'937	91.76	34.82
C171Y_1.2	C171Y/+	1	6'435	95.13	35.73
C171Y_1.3	C171Y/+	1	5'301	91.87	34.83
R186S_1.1	R186S/+	1	5'132	92.7	35.07
R186S_1.2	R186S/+	1	4.891	92.81	35.07
R186S_1.3	R186S/+	1	5'212	89.28	34.22
WT_4.1	+/+	4	6'592	90.15	34.45
WT_4.2	+/+	4	7'648	91.63	34.75
WT_4.3	+/+	4	8'959	93.77	35.42
C171Y_4.1	C171Y/+	4	6'932	92.41	35.01
C171Y_4.2	C171Y/+	4	9'851	93.28	35.36
C171Y_4.3	C171Y/+	4	7'213	92.23	34.97
R186S_4.1	R186S/+	4	6'392	91.81	34.79
R186S_4.2	R186S/+	4	6'809	91.74	34.72
R186S_4.3	R186S/+	4	5'311	91.77	34.98

All reads have passed the Illumina chastity filter. %Q30, percentage of bases with quality score ≥30; Mean Q, prediction of the probability of a wrong base call.

Appendix References

Dahan K, Devuyst O, Smaers M, Vertommen D, Loute G, Poux JM, Viron B, Jacquot C, Gagnadoux MF, Chauveau D *et al* (2003) A cluster of mutations in the UMOD gene causes familial juvenile hyperuricemic nephropathy with abnormal expression of uromodulin. *J Am Soc Nephrol* 14(11):2883-93.

Ioannidis NM, Rothstein JH, Pejaver V, Middha S, McDonnell SK, Baheti S, Musolf A, Li Q, Holzinger E, Karyadi D *et al* (2016) REVEL: An Ensemble Method for Predicting the Pathogenicity of Rare Missense Variants. *Am J Hum Genet* 99(4):877-85.

Karczewski KJ, Francioli LC, Tiao G, Cummings BB, Alföldi J, Wang Q, Collins RL, Laricchia KM, Ganna A, Birnbaum DP *et al* (2020) The mutational constraint spectrum quantified from variation in 141,456 humans. *Nature* 581(7809):434-43.

Kopanos C, Tsiolkas V, Kouris A, Chapple CE, Albarca Aguilera M, Meyer R, Massouras A (2019) VarSome: the human genomic variant search engine. *Bioinformatics* 35(11):1978-80.

Turro E, Astle WJ, Megy K, Gräf S, Greene D, Shamardina O, Allen HL, Sanchis-Juan A, Frontini M, Thys C *et al* (2020) Whole-genome sequencing of patients with rare diseases in a national health system. *Nature* 583(7814):96-102.

Van Hout CV, Tachmazidou I, Backman JD, Hoffman JD, Liu D, Pandey AK, Gonzaga-Jauregui C, Khalid S, Ye B, Banerjee N *et al* (2020) Exome sequencing and characterization of 49,960 individuals in the UK Biobank. *Nature* 586(7831):749-56.